ADVANCED HEALTHCARE MATERIALS
www.advhealthmat.de

Stimuli-Mediated Macrophage Switching, Unraveling the Dynamics at the Nanoplatforms–Macrophage Interface

*Keya Ganguly, Rachmi Luthfikasari, Aayushi Randhawa, Sayan Deb Dutta, Tejal V. Patil, Rumi Acharya, and Ki-Taek Lim**

Macrophages play an essential role in immunotherapy and tissue regeneration owing to their remarkable plasticity and diverse functions. Recent bioengineering developments have focused on using external physical stimuli such as electric and magnetic fields, temperature, and compressive stress, among others, on micro/nanostructures to induce macrophage polarization, thereby increasing their therapeutic potential. However, it is difficult to find a concise review of the interaction between physical stimuli, advanced micro/nanostructures, and macrophage polarization. This review examines the present research on physical stimuli-induced macrophage polarization on micro/nanoplatforms, emphasizing the synergistic role of fabricated structure and stimulation for advanced immunotherapy and tissue regeneration. A concise overview of the research advancements investigating the impact of physical stimuli, including electric fields, magnetic fields, compressive forces, fluid shear stress, photothermal stimuli, and multiple stimulations on the polarization of macrophages within complex engineered structures, is provided. The prospective implications of these strategies in regenerative medicine and immunotherapeutic approaches are highlighted. This review will aid in creating stimuli-responsive platforms for immunomodulation and tissue regeneration.

1. Introduction

Recently, there has been tremendous development in immunomodulatory therapies for life-threatening diseases such as cancer and diabetes.[1,2] Immunomodulatory drugs are used to modulate the immunological response of patients by enhancing or diminishing certain activities of the body's immune system.[3] Various pharmaceutical agents are designed to target any of the immune cells, i.e., natural killer cells, cytotoxic T-lymphocytes, lymphocytes, neutrophils, and macrophages. Among these, macrophages derived from blood monocytes are extensively researched for immunotherapy, given their pivotal function in both innate immune response and tissue remodeling.[4,5] In brief, macrophages have unique adaptability and can assume many functional phenotypes typically categorized into proinflammatory (M1) and anti-inflammatory (M2) states. This phenomenon is often called macrophage polarization.[6–9] It is known that under certain circumstances, these distinct macrophage phenotypes can potentially undergo reciprocal transformations.[10,11] The designations "M1" and "M2" were chosen to reflect the distinct effects these two macrophage populations induce on differentiating T-lymphocytes. M1 macrophages are distinguished by their capacity to direct and stimulate Th1 T-lymphocytes; conversely, M2 macrophages are associated with producing Th2 T-lymphocyte responses.[12]

M1 macrophages can be stimulated by various factors, including lipopolysaccharide (LPS), interferon-gamma (IFN-γ), tumor necrotic factor-alpha (TNF-α), and granulocyte–macrophage colony-stimulating factor.[13] M1-polarized macrophages lead to the clearance of pathogens through the production of nitric oxide (NO), reactive oxygen species (ROS), and reactive nitrogen species.[14] Additionally, M1 macrophages exhibit elevated expression of antigen-presenting major histocompatibility complex (MHC) complexes, thereby activating adaptive immune responses.[15] Conversely, M2 macrophages are propelled toward tissue restoration by interleukin 4 (IL-4) and IL-13, interleukins secreted by innate and adaptive immune cells, including basophils, mast cells, and Th2-lymphocytes.[16] M2 macrophages are further characterized into M2a, M2b, M2c, and

K. Ganguly, R. Luthfikasari, A. Randhawa, S. D. Dutta, T. V. Patil, R. Acharya, K.-T. Lim
Department of Biosystems Engineering
Kangwon National University
Chuncheon 24341, Republic of Korea
E-mail: ktlim@kangwon.ac.kr

K. Ganguly
Institute of Forest Science
Kangwon National University
Chuncheon 24341, Republic of Korea

A. Randhawa, T. V. Patil, R. Acharya, K.-T. Lim
Interdisciplinary Program in Smart Agriculture
Kangwon National University
Chuncheon 24341, Republic of Korea

The ORCID identification number(s) for the author(s) of this article can be found under https://doi.org/10.1002/adhm.202400581

DOI: 10.1002/adhm.202400581

M2d subgroups based on their surface markers, secreted cytokines, and function regarding various stimulating molecules or microenvironments.[17,18] Variations in macrophage phenotypes (M1, M2, and M2 subtypes) can be measured using the cell secretome and several cell surface markers (**Table 1**). According to previous research, M2a macrophages secrete large amounts of IL-4 and IL-13 and overexpress mannose receptor C-type 1, a cluster of differentiation 206 (CD206) and fibronectin, which promotes wound healing.[19,20] M2b macrophages secrete important anti-inflammatory cytokines that promote B lymphocyte activation and humoral immunity.[21] M2c macrophages trigger anti-inflammatory responses through IL-10 signaling and efficiently phagocytose apoptotic cells by overexpressing Mer receptor tyrosine kinase (MerTK).[22] M2d macrophages express high levels of vascular endothelial growth factor (VEGF), IL-10, and TGF-β and play a crucial role in tissue sarcoma as the key inflammatory inducers. Additionally, it encourages angiogenesis and cancer progression.[23–25] Regardless of the circumstance, M2 macrophages repair tissue and inhibit M1 activity.[26–30]

The ability to manipulate macrophage polarization toward the desired phenotype has enormous therapeutic implications in tissue engineering,[31,32] regenerative medicine,[33,34] and immunotherapy.[35,36] Multiple methods are available to induce the polarization of macrophages into one of two functional states, in vitro and in vivo. Among these, the integrated effect of external physical stimulation and engineered micro/nanoplatforms has demonstrated encouraging results.[37,38] The dynamic macrophage polarization is ideally achieved by external stimulation when using micro/nanoplatforms since these specifically engineered platforms enhance the transmission of such stimuli to cells.[39] One instance involves the utilization of micro/nanostructured platforms that possess topographical cues, including fissures, pillars, and nanofibers. The ability of these platforms to facilitate the regulated transmission of external stimuli to macrophages stems from their distinctive capability to initiate diverse signal transduction pathways recognized by focal adhesion complexes at the material–cell biointerface.[64–67] Surface chemistry alterations, such as coating biomolecules, may further affect stimulation transmission and dynamic macrophage polarization.[67–69]

Comprehensive reviews have investigated the impact of external signals on macrophage polarization and the role of biomimetic structures in regulating dynamic polarization separately.[70,71] However, reviewing current research on stimuli and tailored platforms for macrophage polarization is crucial, given their significant role at the intersection of biology and engineering. It has implications for high-throughput immunotherapy and tissue regeneration. Combining stimuli with complex structures provides new insights into macrophage behavior, advancing our understanding and potential impact in this field.

This review examines the most recent advancements in the engineered platforms regulating macrophage polarization combined with external stimulation for therapeutic and tissue engineering applications (**Scheme 1**). The structural–functional aspect of designed platforms and the molecular mechanisms that regulate the interaction between stimuli and biomimetic structures in the dynamics of macrophage modulation are emphasized. Finally, a summary of the most recent reports on the clinical implementation of the developed systems is also presented. We anticipate that this work provides a comprehensive overview of the current state of this field.

2. Macrophage Polarization

The process of macrophage polarization is a multifaceted and dynamic phenomenon regulated by numerous molecular processes and signaling pathways.[72,73] The consideration of potential metrics for assessing macrophage polarization remains a challenging task. However, estimating macrophage polarization is frequently achieved by observing certain hallmark changes, including alterations in genetic[13] and proteomic marker expression,[81] cytokine/chemokine secretions,[82] and interactions with neighboring cells.[83] Additionally, metabolic factors[84] and epigenetic modifications[85] regulate macrophage polarization. The intricate interplay of these factors dictates the polarization state of macrophages, which influences their functional phenotype and responses in physiological and pathological contexts (**Scheme 2a**). Furthermore, macrophage polarization dynamics often provide a momentary representation unique to the present microenvironment, increasing the complexity of the study of polarization.[9]

2.1. Signaling Pathways in Macrophage Polarization

Since macrophage polarization is governed by specific signaling pathways that cause phenotypic and biochemical changes, this section summarizes the main signaling pathways that genetically control macrophage polarization.

2.1.1. Toll-Like Receptor (TLR) Signaling

Toll-like receptors (TLRs) are essential pattern recognition receptors that identify pathogen-associated molecular patterns (PAMPs) and initiate immune responses.[86,87] Engagement of TLRs on macrophages triggers signaling cascades, including TIR-domain-containing adapter-inducing interferon-β-dependent pathways and myeloid differentiation primary response 88 (MyD88)-dependent cascade, which produce proinflammatory cytokines and chemokines.[88] TLRs initiate intracellular signaling cascades that ultimately result in the activation of transcription factors and the production of specific cytokines and chemokines upon ligand binding, promoting both M1 and M2 polarization, depending on the TLR agonist and environmental conditions. For instance, LPS in gram-negative bacteria stimulates the production of proinflammatory cytokines such as IL-6 and TNF-α, resulting in M1 polarization.[89] TLR2 activation by molecules from bacteria, fungi, or other microbial components[90,91] and TLR3 activation by double-stranded RNA can induce the expression of anti-inflammatory cytokines, including IL-10 and TGF-β, thereby promoting M2 polarization.[92–94] In addition, TLR signaling can influence other signaling pathways, such as those involving interferon-gamma (IFN-γ) or IL-4, to further influence macrophage polarization.[7,95–98]

Table 1. A comprehensive list of M1 and M2 macrophage markers along with their roles.

Macrophage type/subtype	Key markers	Surface markers	Secreted factors	Immune response	Tissue healing	Refs.
M1	CD86, CD80, CD40, CD64	CD11b, CD14, CD16, CD32	Tumor necrosis factor-alpha (TNF-α)	Proinflammatory response, microbicidal activity, increased phagocytosis, antigen presentation, T-helper1 (Th1) response	Promotes early inflammation, clears pathogens, stimulates tissue repair and remodeling, angiogenesis, and fibrosis	[16, 40, 41]
	iNOS (inducible nitric oxide synthase)		Interleukin-1 beta (IL-1β) Interleukin-6 (IL-6) Interleukin-12 (IL-12) Interferon gamma (IFN-γ)			[42–45]
M2	CD206 (mannose receptor)	CD163, CD204, CD209, CD200R	Interleukin-10 (IL-10)	Anti-inflammatory response, T-helper 2 (Th2) response, increased tissue remodeling, tissue repair, and regeneration	Resolves inflammation, promotes tissue remodeling and repair, wound healing, promotes angiogenesis, dampens immune response	[45–47]
	Arg-1 (arginase-1)		Transforming growth factor-beta (TGF- β) Interleukin-4 (IL-4) Interleukin-13 (IL-13) Chemokine (C–C motif) Ligand 22 (CCL22)	Suppress NO-induced cytotoxicity, promote fibrosis and collagen synthesis, enhances cell proliferation	Anti-inflammation, cell proliferation	[48–52]
M2a	CD206, CD163, CD209, CD200R, Arg-1	IL1Ra, IL1R II, Arg-1, FIZZ1, Ym1/2	TGF-β, CCL17, CCL18, CCL22, CCL24, Th2 (anti-inflammatory cytokine)	Enhances proliferation of nonmyeloid cells, deactivates M1 phenotype	Tissue repair and remodeling, anti-inflammatory response, phagocytosis, collagen synthesis, fibroblast proliferation	[53–57]
M2b	CD86, CD36, CD163, TLRs, IL-1R8	IL-10 high, IL-12 low, CD86	IL-10, IL1β, IL-6, TNF-α	Induces both anti- and proinflammatory cytokines	Damping of the immune response, immunomodulation, immune regulation, antigen presentation	[58, 59]
M2c	CD163, CD209, CD206, CD36, MerTK	TLR-1, TLR-8, Mouse, Arg-1	IL-10, TGF-β, CCL16	Anti-inflammatory against apoptotic cells	Resolution of inflammation, tissue repair, scavenging debris, phagocytosis, anti-inflammatory response	[22, 58]
M2d	CD206, CD16, CD163, CD14, CX3CR1	VEGF, IL-12 low, TNF-α low, IL-10 high	VEGF, IL-10	Tumor progression, angiogenic	Tumor promotion, immunosuppression, angiogenesis, tissue remodeling	[24, 60, 61]
M2-like (tumor-associated macrophage)	CD206, CD163, CD14, CD204, CD163, CD200R	IL-12 low, IL-10			Tumor promotion, immunosuppression, angiogenesis, tissue remodeling	[62, 63]

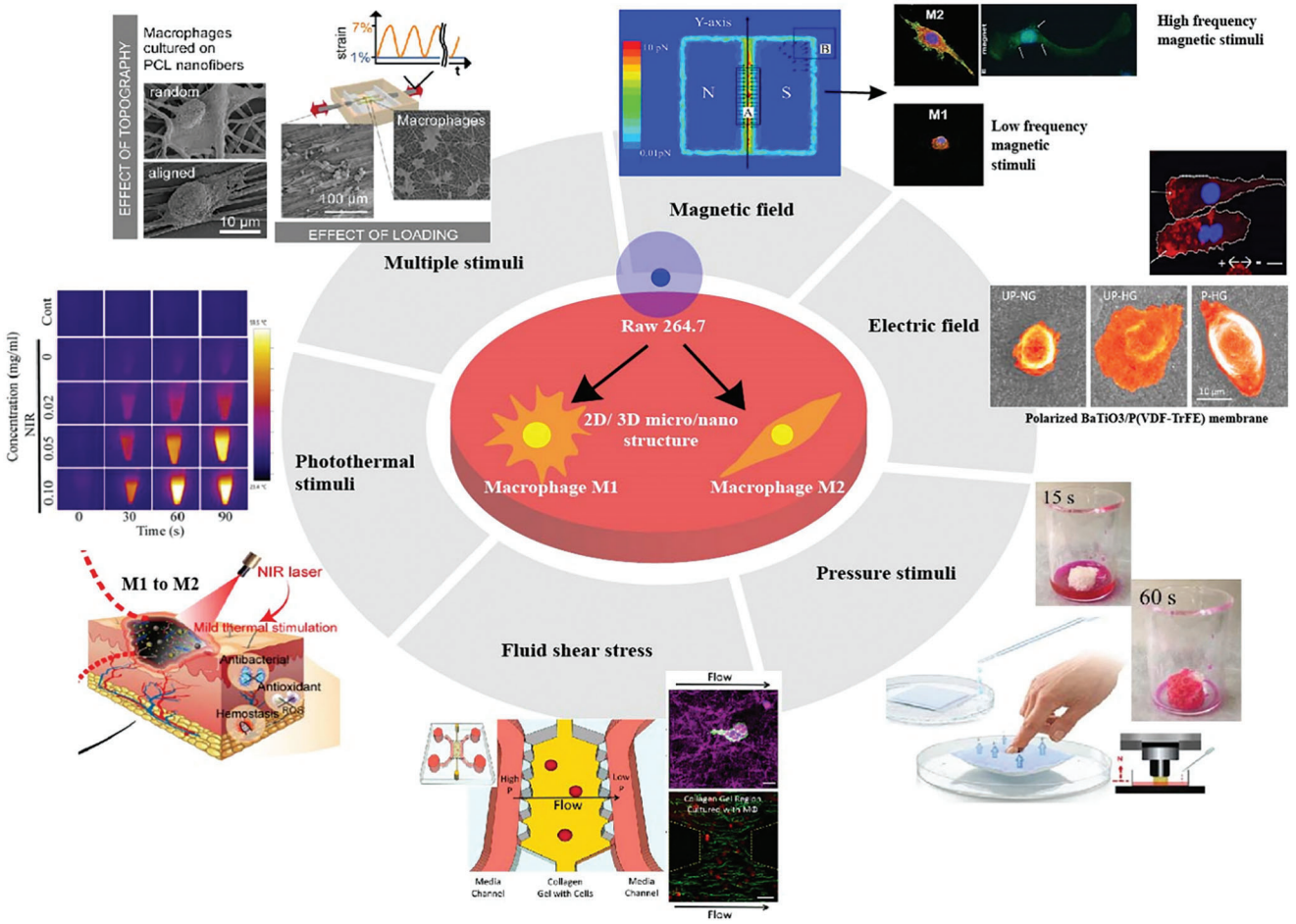

Scheme 1. Overview of the immunomodulatory potential of the combined effects of micro/nanoplatforms' physiochemical properties, and externally applied physical stimulations, including magnetic field. Reproduced with permission.[74] Copyright 2017, American Chemical Society; Electric field, Reproduced under the terms of the CC-BY 4.0 license.[75] Copyright 2021, the Authors, published by Elsevier; Pressure stimuli, Reproduced with permission.[76] Copyright 2023, Elsevier; Fluid shear stress, Reproduced under the terms of the CC-BY 4.0 license.[77] Copyright 2018, the Authors, published by The American Society for Cell Biology; Photothermal stimulation, Reproduced with permission.[78,79] Copyright 2022 and 2020, Elsevier; Multiple stimulation, Reproduced with permission.[80] Copyright 2020, Elsevier., on the macrophage polarization toward M1 or M2 phenotypes when cultured on 2D/3D micro/nanofabricated tissue engineering platforms.

2.1.2. Interferon (IFN) Signaling

Interferons (IFNs), including type I (IFN-α and IFN-β) and type II interferons (IFN-γ), are important cytokines that regulate immune responses.[99] These are produced by various cell types, including macrophages, in response to bacterial or viral infection, tumor development, or other immune stimulatory signals.[100,101] IFN exerts its effects on macrophage polarization by activating specific signaling pathways. IFN-γ mainly activates the Janus kinase (JAK)/signal transducer and activator of the transcription (STAT) signaling pathway upon binding to its receptor. Upon IFN binding to their respective receptors on the macrophage surface, JAK proteins are activated and phosphorylate the cytoplasmic tails of the receptor subunits. This phosphorylation event allows recruitment and phosphorylation of STAT proteins, primarily STAT1 and STAT3. Phosphorylated STATs dimerize and translocate to the nucleus, where they bind to specific DNA elements known as interferon-stimulated response elements (ISREs) or gamma-activated sequence (GAS) elements[102–105] and primarily induce the expression of proinflammatory genes associated with the ISRE and GAS elements.[13,106] Specifically, IFN-γ promotes M1 polarization by producing high levels of ROS and NO through the upregulation of inducible nitric oxide synthase (iNOS) and NADPH oxidase.[107–109] Furthermore, IFN signaling enhances the antigen presentation capabilities of macrophages by upregulating major histocompatibility complex class I (MHC-I) and class II (MHC-II) molecules.[110] This facilitates the activation of adaptive immune responses. Interferon signaling can also modulate M2 macrophage polarization through the involvement of interferon-regulatory factors (IRFs).[111]

2.1.3. IL-4/IL-13 Cytokine Receptor Signaling

IL-4 and IL-13 are essential cytokines for the induction of M2 polarization.[112,113] The binding of IL-4/IL-13 to their receptors

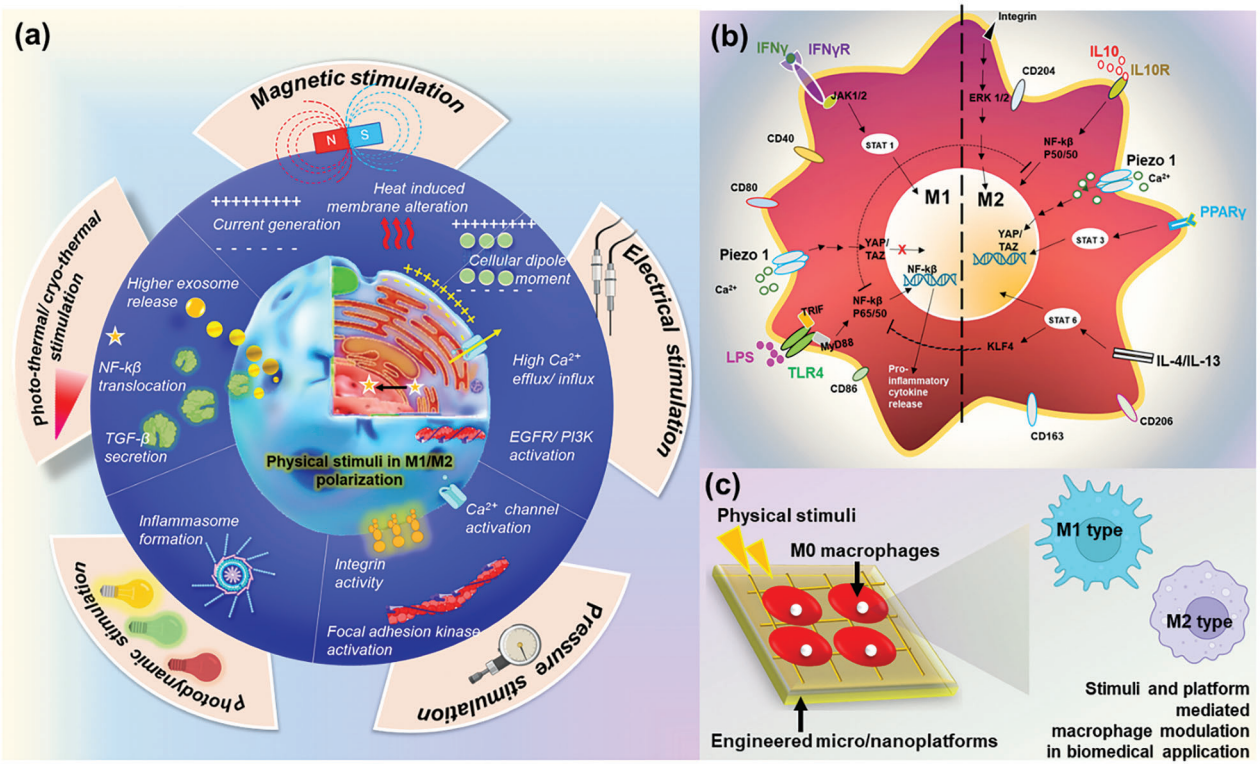

Scheme 2. Schematic illustration of a) the effects of physical stimulation on the behavior of macrophage polarization. b) Key signaling pathways altered in dynamic macrophage polarization. c) The advancement in the micro/nanoplatform device coupled with external physical stimulation for dynamic macrophage polarization.

activates the JAK/STAT6 pathway.[103,114] STAT6 has been reported to translocate to the nucleus and promote M2-specific genes, including arginase-1 (Arg-1), mannose receptor (CD206), TGF-β, and anti-inflammatory cytokines such as IL-10.[115] These cytokines exert immunoregulatory effects, suppressing proinflammatory responses and promoting tissue repair and resolution of inflammation.[116]

IL-4/IL-13-stimulated M2 macrophages perform essential tissue remodeling and wound healing functions through extracellular matrix (ECM) deposition, angiogenesis, and tissue repair,[117,118] mainly through increased matrix metalloproteinase (MMP) production by M2 macrophages.[119] IL-4/IL-13-driven M2 macrophages display immunoregulatory functions that promote immune tolerance and suppress excessive immune responses.[120,121] Contributing to immune homeostasis and regulation, other immune cells can inhibit proinflammatory cytokine production and promote the differentiation of regulatory T cells (T_{regs}).[122] Furthermore, tumor-associated macrophages (TAMs) tend to polarize toward an M2-like phenotype under the influence of IL-4/IL-13 signaling, which mediates their immunosuppressive properties. This polarization is commonly associated with tumor progression, angiogenesis, and immune evasion within the tumor microenvironment.[123]

Hence, IL-4/IL-13 signaling promotes the M2 or alternative activation phenotype during macrophage polarization. This pathway produces anti-inflammatory cytokines, tissue-remodeling factors, and immunoregulatory molecules contributing to wound healing, tissue repair, immunoregulation, and tumor progression.

2.1.4. Nuclear Factor-Kappa B (NF-κB) Signaling

Transcription factor NF-κB signaling plays a significant role in macrophage polarization by regulating the gene expression involved in inflammatory and immune responses.[124,125] Upon activation, NF-κB induces the transcription of proinflammatory cytokines such as TNF-α, IL-1β, and IL-6.[126] It acts as a downstream effector of TLR signaling. Upon activation of TLRs by PAMPs or danger-associated molecular patterns, NF-κB activation leads to the expression of iNOS, producing NO and ROS. These molecules are involved in pathogen clearance and the inflammatory response.[127] NF-κB signaling also interacts with IFN-γ and IL-4 signaling pathways, where IFN-γ enhances NF-κB activity, promoting M1 phenotypic change, while IL-4/IL-13 signaling suppresses NF-κB activity favoring, M2 polarization.[125] NF-κB mediated signaling also plays a key role in the resolution of inflammation through IL-10 and TGF-β signaling.[128]

2.1.5. Peroxisome Proliferator-Activated Receptor-Gamma (PPAR-γ) Signaling

PPAR-γ is a nuclear receptor that controls lipid metabolism and immune responses.[129] Activation of PPAR-γ by PPAR-γ

agonists, such as thiazolidinediones, promotes the expression of IL-10 and suppresses the production of proinflammatory cytokines, such as TNF-α and IL-6,[130,131] fostering an immunoregulatory M2 phenotype.

PPAR-γ signaling exerts anti-inflammatory, immunoregulatory, and tissue-remodeling effects while regulating glucose and lipid metabolism.[132] PPAR-γ signaling regulated lipid metabolism in macrophages promotes lipid uptake, efflux, and metabolism and contributes to the formation of M2-like cells.[133,134] Activation also regulates lipid balance, mitigating lipid-induced inflammation by promoting lipid accumulation and droplet formation.[135] M2 macrophages induced by PPAR-γ activation are involved in ECM deposition, angiogenesis, and tissue repair.[136] Furthermore, PPAR-γ signaling interacts with other pathways involved in macrophage polarization, including IL-13/IL-4 signaling, enhancing M2 polarization. PPAR-γ activation can also modulate TLR signaling and suppress the proinflammatory response associated with M1 polarization.[137]

2.1.6. Signal Transducer and Activator of Transcription 3 (STAT3) Signaling

STAT3 is a TF activated by numerous cytokines and growth factors. STAT3 activation stimulates the gene expression associated with M2 and contributes to anti-inflammatory functions, mostly through IL-6, IL-10, and IL-13 signaling,[138] and inhibits the production of proinflammatory cytokines, such as TNF-α, IL-1β, and IL-6. It also modulates the function of regulatory T cells (T_{regs}) and regulatory B cells (B_{regs}), promoting an anti-inflammatory environment and suppressing excessive immune responses.[139,140] This suppression of proinflammatory gene expression contributes to the resolution of inflammation and restoration of immune homeostasis.[104,141]

2.2. Macrophage Polarization under Physical Stimulation(s)

How does physical stimulation influence macrophage polarization, and what are its hallmarks? Given the overlapping molecular pathways implicated in macrophage polarization, providing a direct answer to this inquiry is exceedingly difficult. Moreover, it is essential to acknowledge that the impact of external stimulation on cells might exhibit variability depending upon the intensity, frequency, and length of exposure alongside the specific cellular and organismal entities under consideration. Consequently, the regulation of immune cells like macrophages and the homogeneity of the regulatory mechanisms are yet to be explored, and extensive data deposition through databases like the ImmGen consortium can help to surmount these challenges.[142]

2.2.1. Magnetic/Electromagnetic Stimulation

The exposure of macrophages to a static or dynamic magnetic field (MF) can differentially enhance a cell's magneto reception, induce current generation, alter membrane properties, and generate heat, resulting in alteration in various cellular processes. For instance, Vergallo et al. demonstrated that exposure to a strong, homogenous static MF of 476.7 ± 0.1, 12.0 ± 0.1, 2.8 ± 0.1 for up to 24 h has a significant inhibitory effect on the release of proinflammatory cytokines IL-6, IL-8, and TNF-α from Raw 264.7 macrophages.[143] On the contrary, a pulsed MF can modulate excessive inflammatory reactions in an in vivo setup. Kim et al. have demonstrated that exposure of BALB/c + LPS mice exposed to a pulsed MF of 4700 G greatly reduces the expression of proinflammatory cytokines, TNF-α levels, and IL-6.[144] Similar macrophage behavior results when Raw 264.7 + LPS are exposed to a varying MF of 30 Hz for 1 h in an in vitro setup; the MF induces a decrease in the secretion of IL-6 and IL-10 without altering the production of TNF-α.[145] More or less, exposure to MFs may promote M2 polarization of macrophages. However, a distinct behavioral pattern happens when macrophages are exposed to electromagnetic fields (EMFs). Kim et al. observed that the exposure of Raw 264.7 cells to 60 Hz 0.8 mT low-frequency EMF increased the production of proinflammatory cytokines, TNF-α, IL-1β, and IL-6 without altering the cell proliferation behavior. It also resulted in increased NF-kβ signaling, enhanced activation of nuclear factor of activated T cells (NFAT)2, and an increased influx of calcium, and resulted in a decreased effectiveness of antioxidants like Resveratrol.[146] MF also affects the phagocytic capability of macrophages. Macrophages derived from Shoe-NMRI mice upon exposure to 50 Hz MF at 1.0 mT were investigated for uptake behavior. MF-exposed macrophages showed a 1.6-fold increased uptake of latex beads within 45 min. Additionally, these macrophages released an increased IL-1β after 24 h of 1.0 mT MF exposure.[147] The effects of MF in an in vivo system are quite different. BALB/c male mice, when exposed to weak combined MFs produced by a constant MF (30–150 μT) and an alternating MF (100 or 200 nT) for 2 h daily for 14 days, can stimulate the production of TNF-α, IFN-γ, IL-2, IL-3, and induces cytokine accumulation in blood plasma. A similar treatment can also suppress tumor growth in mice.[148] The polarization of naïve M0 macrophages into the anti-inflammatory M2 phase was significantly impacted by moderate (≈0.6 T) or gradient (≈104 Tm^{-1}) MF, according to multiple studies conducted to date. It has been demonstrated that MF enhances the expression of anti-inflammatory genes in macrophages by activating STAT6 and inhibiting STAT1, thereby promoting the resolution of inflammation and the healing of wounds.[149] Lei et al. have described the possible mechanism of MF interaction with macrophage biology. Exposure of macrophages to an external MF initiates a series of intracellular responses, including rearrangements in the actin cytoskeleton, the Golgi complex, and the cation channel receptor transient receptor potential cation channel, subfamily M, member 2 (TRPM2) (**Figure 1**a). The intracellular and intercellular free radicals and molecules, such as O_3, NO, NO_2, and $FeCl_3$, are paramagnetic and can be redistributed by the Lorentz force and the magnetic gradient force as defined in electrochemistry. It is also known that exposure of the macrophages to an external MF induces clustering of cation channel receptor TRPM2 to disrupt the Ca^{2+} homeostasis, resulting in reoriented ion-current dependent actin polymerization and reshaping the cells. Moreover, MF alters the interaction of actin-binding molecules such as vinculin, mitotic spindles, and chromosomes. An alternating MF and ultrahigh MF also strongly influence the spin (charge) transfer between ions due to the strong natural magnetic moments of Fe

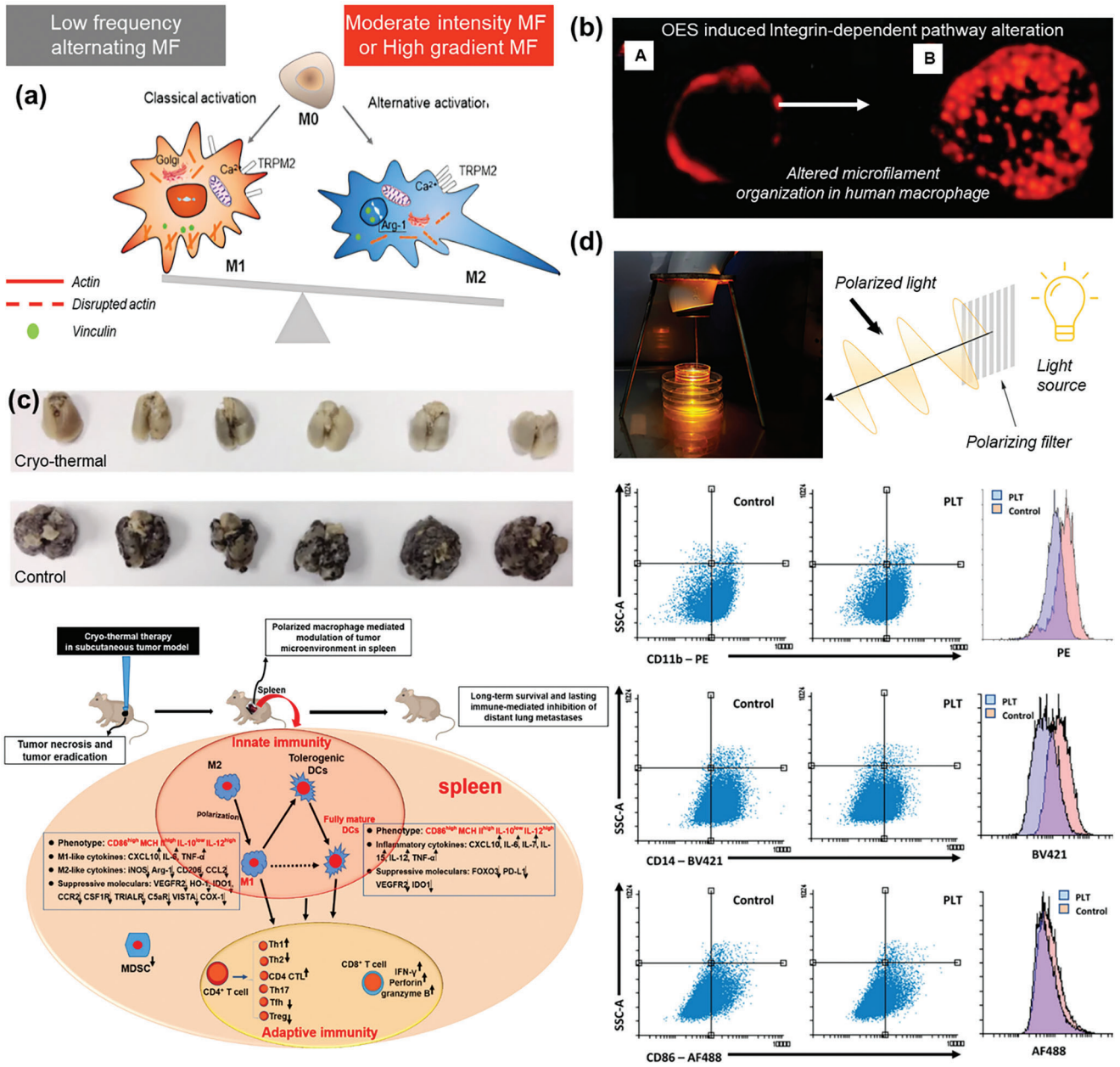

Figure 1. Effects of physical stimuli on macrophage polarization. a) Macrophage shift to M1 phenotype with low-frequency alternating magnetic field and to M2 phenotype with moderate intensity MF, potentially resulting from TRPM2 clustering mediated Ca^{2+} homeostasis and actin polymerization, Golgi complex disruption, and activation of M2 specific gene Arginase-1. Reproduced under the terms of the CC-BY 4.0 license.[149] Copyright 2020, Frontiers. b) Changed microfilament organization. Reproduced with permission.[150] Copyright 2000, Springer Nature. c) Illustration depicting cryothermal therapy's induction of M1 phenotype in macrophages, leading to the remodeling of the host immune environment and the initiation of long-lasting antitumor memory immunity. Reproduced under the terms of the CC-BY 4.0 license.[151] Copyright 2019, Springer Nature. d) U937 macrophages exposed to polarized light stimulation and the resulting reduced inflammatory marker expression. Reproduced with permission.[152] Copyright 2020, Wiley.

atoms and ions.[149] MF exposure thus promotes M2 macrophage polarization at several experimental instances over M1 states.

2.2.2. Electrical Stimulation

Cells exposed to an external electric field (EF) often experience induced dipole moments, creating a difference in the polarization potential, enhanced cell cathode migration, and alignment to EF vectors, mainly through epidermal growth factor receptor, phosphoinositide 3-kinase (PI3K), and Ca^{2+}-related mechanisms.[153] It was observed a long time ago that applying an external EF of 150 mV mm^{-1} for a period of 2 h induces anodal migration of macrophages without increasing the speed or direction of migration. In addition, this stimulation can polarize polymerized actin and podosome toward the leading, anode-facing edge

and enhance their phagocytic ability. Interestingly, exposure of the progenitor monocytes of these macrophages showed a directional migration toward the cathode. This stimulation condition increases PI3K and extracellular signal-regulated kinase (ERK) activities. However, they will likely not activate the STAT3 and the p38 activities. Investigations using inhibitors for PI3K, ERK, and Ca^{2+} signaling show that integration of multiple pathways is required to drive EF-mediated effects fully.[154] Macrophages, when cultured on glass substrates and exposed to an oscillatory EF of 1 Hz, 2 V cm^{-1}, can attain an induced migration velocity of 5.2 $\pm$ 0.4 $\times$ 10^{-2} µm min^{-1} through integrin-dependent or integrin-independent signaling pathways (Figure 1b).[150]

2.2.3. Photothermal/Cryothermal Stimulation

Macrophage polarization also responds to variations in temperature. In conditions such as fever, the BALB/c mice model challenged with LPS shows enhanced signaling pathways, including enhanced phosphorylation of the inhibitor of nuclear factor-κB kinase complex, resulting in NF-κB nuclear translocation and binding to TNF-α promoter. Interestingly, this expression of TNF-α is tightly connected to the expression of heat shock protein 70 (HSP70), whose inhibition can lead to lower the expression of TNF-α.[155] The effect of heat can indirectly control the macrophage polarization process in several instances. For example, when exposed to hyperthermia, triple-negative breast cancer cell lines release exosomes that affect macrophage polarization. Hyperthermia-treated MDA-MB-231 human breast cancer cells secrete HSPB8-containing exosomes readily upregulate the mRNA levels of TAM M1 marker IL-12 and iNOS while downregulating the M2 markers CD206 and Arg-1. The release of M1 polarizing exosome occurs through the enhanced MAPK, TNF, and IL-17 signaling pathways.[156] On the contrary, cryothermal therapies can also increase the expression in CD 86, MHC-II, CXCL 10, IL-12p40, IL-6, and TNF-α mRNA levels, as investigated in female C57BL/6 mice. Cryothermally polarized M1 macrophages can be crucial in dendritic cell (DC) activation and maturation, leading to antitumor CD4+ and cytotoxic CD8+ T-cell activation. Figure 1c depicts the emergence of M1 phenotype macrophage utilizing cryothermal treatment, resulting the modification of the host immunological milieu and onset of persistent antitumor memory immunity.[151] Thermal treatment of the macrophages and implantable biomaterial can have a different effect as opposed to the M1 polarization tendencies of heat stimulation, a near-infrared (NIR) treatment of mice implanted with antioxidized polydopamine@hydroxyapatite (2PDA@HA) with photothermal treatment (808 nm, 0.75 W cm^{-1}) promotes macrophage polarization toward the M2 state by secreting platelet-derived growth factor-BB (PDGF-BB) and TGF-β1.[157]

2.2.4. Photodynamic Stimulation

Control of macrophage polarization using unpolarized light stimulation is another way toward immunomodulation. Light stimulation has been shown to trigger the expression of cyclooxygenase 2, prostaglandin E2, TLR 4, and triggering receptor expressed on myeloid cells 1 (OCX2/PGE2/TLR4/TREM1) axis to induce M1 macrophage polarization in THP-1 macrophages.[158] Besides, photodynamic therapy (PDT) also triggers the expression of Arg-1, CD 206, iNOS, CD86, inflammatory factor IL-6, TNF-α, and IL-β1, MAPK/ERK pathway activation, and NOD-like receptor protein 3 (NLRP3) inflammasome formation.[159] Histiocytic lymphoma cell line U-937, when subjected to light at 660, 820, 870, and 880 nm, results in the differential secretion of growth factors that affect fibroblast proliferation differentially. Another way to control macrophage polarization is the use of polarized light. Human monocyte cells U937, upon exposure to polychromatic polarized light for 6 h, often result in a reduced expression of CD14, MHC-I, and CD11b receptors while increasing the expression of CD86 (Figure 1d). It also downregulates IL1B, chemokine (C–C motif) ligand 2 (CCL2), NLR family pyrin domain containing 3 (NLRP3), and nucleotide-binding oligomerization domain-containing protein 1 (NOD1) while upregulating NFKBIA and TLR9. NFKBIA is a key inflammatory inhibitor of cytokine production. IL1B and CCL2 are important cytokines, while NLRP3 and NOD1 are membrane receptors in inflammatory signaling.[152] Photobiomodulation treatment with 630 nm light emitting diode array on a coculture system of Raw 264.7 cells and Tonsil-derived mesenchymal stem cells at 30J reduces expression of iNOS (M1) and increases the expression of Arg-1 (M2) phenotype macrophage markers. Anti-inflammatory cytokines interleukin-1 receptor antagonist (IL-1RA) gene expression also increases significantly.[160]

2.2.5. Pressure Stimulation/Mechano-Immunomodulation

Macrophages are mechanically responsive and can alter their lineages according to mechanical stimuli surrounding them. Tensile micromechanical strains, hydrostatic cyclic pressure, and compressive strains are known to accelerate inflammatory cytokine production. Macrophages also respond to interstitial fluid shear stress by selective release of matrix metalloproteinases (MMPs), leading to ECM degradation and heart diseases. Nevertheless, the polarization state of the macrophage greatly depends on the type of mechanical stimuli, such as low/oscillatory/static shear stress uniaxial and biaxial stretching-induced mechanical stress.[161] These stimuli are perceived through the integrins, voltage-gated Ca^{2+} channels, and focal adhesion kinases and transduced through various signaling pathways, including the MAPK, ERK1/2, and JNK pathways.[162] A few notable findings suggest that a high hydrostatic pressure of ≈60 mmHg can polarize bone marrow-derived macrophage to the M1 phenotype by producing TNF-α and IL-10.[163] Most mechanical stress promotes inflammation by producing inflammasome, activating the NF-kB signaling pathway, and suppressing caspase-1 activation.[164] Regardless of the physical stimulation applied, the induction of M1 or M2 macrophage polarization varies widely and is primarily determined by the specific stimulation context.

Leveraging these plasticities, micro/nanoplatforms combined with targeted external stimuli, either alone or in combination, have been widely employed in engineering immunomodulatory platforms. These platforms aim to manipulate the surrounding topological features of macrophages and amplify signal transduction to achieve dynamic macrophage polarization. As will be elaborated upon in the following section, desired

immunomodulatory platforms can be produced by fine-tuning these stimuli. Scheme 2b,c illustrates a simplified overview of the primary signaling pathways involved in macrophage M1/M2 polarization and the utilization of stimulation coupled with platforms for macrophage fate determination.

3. Physical Stimulations for Macrophage Polarization on Advanced Micro/Nanoplatforms

Various techniques are utilized to fabricate micro/nanoplatforms integrated with stimulation modules for the desired immunomodulatory investigations. These include printed platforms,[165,166] microfluidic devices,[167,168] nanobot fabrication,[169,170] electrospun fiber platforms,[171,172] bioreactors,[173,174] and any combination of platforms[175] depending upon the type of stimulation to be applied. For example, applying MF to MF-responsive nanoplatforms can adjust macrophages' surface adhesion attachment, leading to a controlled polarization event. The surface micro–nanoarray structure can also be converted into detectable electrical signals under external electrical stimulation, which can decode the information to the macrophages.[176] Two prevalent approaches are utilized to fabricate surface micro–nanostructures, top-down, and bottom-up. The top-down approach involves breaking down material to obtain nanostructures, whereas a bottom-up approach focuses on assembling molecules into nanostructures.[177] Mold casting and photolithography are the preeminent top-down construction techniques that enable the manipulation of micro/nanoarrays' characteristic parameters and structural morphology. Bottom-up construction techniques typically involve self-assembly phenomena, such as forming patterned nanomaterial structures via electrostatics, magnetism, or intermolecular forces. Notably, the development of intricate surface patterns frequently necessitates utilizing hybrid construction techniques, which involve integrating both top-down and bottom-up approaches.[178,179] These micro–nanostructure could then be utilized for immunomodulatory applications. We have discussed the fabrication of the case specific nanoplatforms along with the immunomodulatory function in the sections below. Nevertheless, stimuli-responsive micro/nanoplatforms and their fabrication and working principles can be studied in detail in the available literature.[65,180–183]

3.1. Magnetic Field Coupled Platforms

In the natural tissue ECM microenvironment, fibronectin, laminin, and collagen proteins create anisotropic random structures that generate network topologies abundant in Arg–Gly–Asp (RGD) sequences to ligate integrin transmembrane cell receptors. The precise control of the interaction between the RGD sequences of the ECM proteins and the macrophages could affect macrophage polarization, which can either be proinflammatory or promote healing. In this regard, Kim et al. emphasized using an MF to control RGD to integrin binding in macrophages for immunomodulation-induced tissue regeneration (**Figure 2a**).[184] In their study, they found that the polarization of macrophages toward M1 or M2 types could be controlled by an MF-responsive platform comprising three components, including RGD-coated gold nanospheres (RGD-GNS), a 1D magnetic nanocylinder (MNC) coated with RGD (RGD-MNC), and a flexible linker molecule (10 000 Da) connecting the RGD-GNS to the RGD-MNC, as shown in Figure 2a(a1,a2). The attachment and detachment of RGD-MNCs on the RGD-GNS-coated 2D material surface were controlled by an externally applied MF of 10^4 Oe (Figure 2a(a3)). The dynamics of the integrin-mediated interaction between macrophages and the ECM were observed by regulating the attachment and detachment of the nanocylinder to the gold nanospheres. When the MF is applied, the assembled system enhances macrophage focal adhesion to nanoplatforms by enhancing the interaction between integrin and RGD, thereby polarizing into M2 macrophages. The interaction between RGD-integrin in macrophages was attenuated in the absence of an MF owing to the disassembly of the RGD-MNC and RGD-GNS system, resulting in lower focal adhesion mediated M1-polarized macrophages, as depicted in Figure 2a(a4,a5). The observed alteration in macrophage polarization via cellular dynamics in response to magnetic fields exemplifies a remotely controlled switch within the magnetic manipulation platform, ultimately dictating macrophage fate. This instance underscores the magnetic field's capacity to reshape macrophage destiny by regulating the topological environment of cells and manipulating integrin-mediated signaling pathways. The molecular control of the MF-induced macrophage polarization in RGD-MNCs on the RGD-GNS-coated 2D material significantly correlates with the previously reported study by Woski et al., who reported that the application of a 1.24 T magnetic field can induce rearrangements in the macrophage focal adhesion through vinculin and cytoskeletal proteins.[185] The cytoskeletal reorganization resembled the RhoA interference phenotype (Figure 2b). A similar study was conducted by Thangam et al., where the authors demonstrated the embellishment of gold nanoparticles (AuNPs) on magnetic nanoparticles (MNPs) by modulating the density of decorated ligand-bearing AuNPs and flexibly coupling them to a substrate at different MNP densities while maintaining a constant macroscopic ligand density. They demonstrated magnetic switching of upward ("Upper Mag") or downward ("Lower Mag") movement of different ligand-AuNPs through elastic elongation and compression of the flexible linker, respectively, by moving MNPs decorated with ligand-AuNPs toward a magnet. The nanoscale arrangement of the ligand was primarily designed as a 2D array to aid in comprehending cellular adhesion regulation by arranging RGD ligand-presenting nanoparticles with varying interparticle spacing and density. These arrangements were examined in both statically and dynamic conditions, at the microscale and macroscopic density, considering factors such as disordering, clustering, and micropatterns. Their current study utilized the movement of ligand-presenting decorated nanostructures to modulate cell adhesion. This is notably distinct from previous approaches and recent research demonstrating the activity of nondecorated ligand-bearing nanoparticles. Using in situ magnetic AFM imaging, they demonstrated in situ magnetic switching of the ligand-bearing AuNP movement via elongation and compression of the flexible linker. Using the molecular switches of myosin II, F-actin, and Rho-associated kinase (ROCK), they demonstrated that the high-density and downward movement of ligand-AuNPs promoted the adhesion-regulated M2 polarization of macrophages

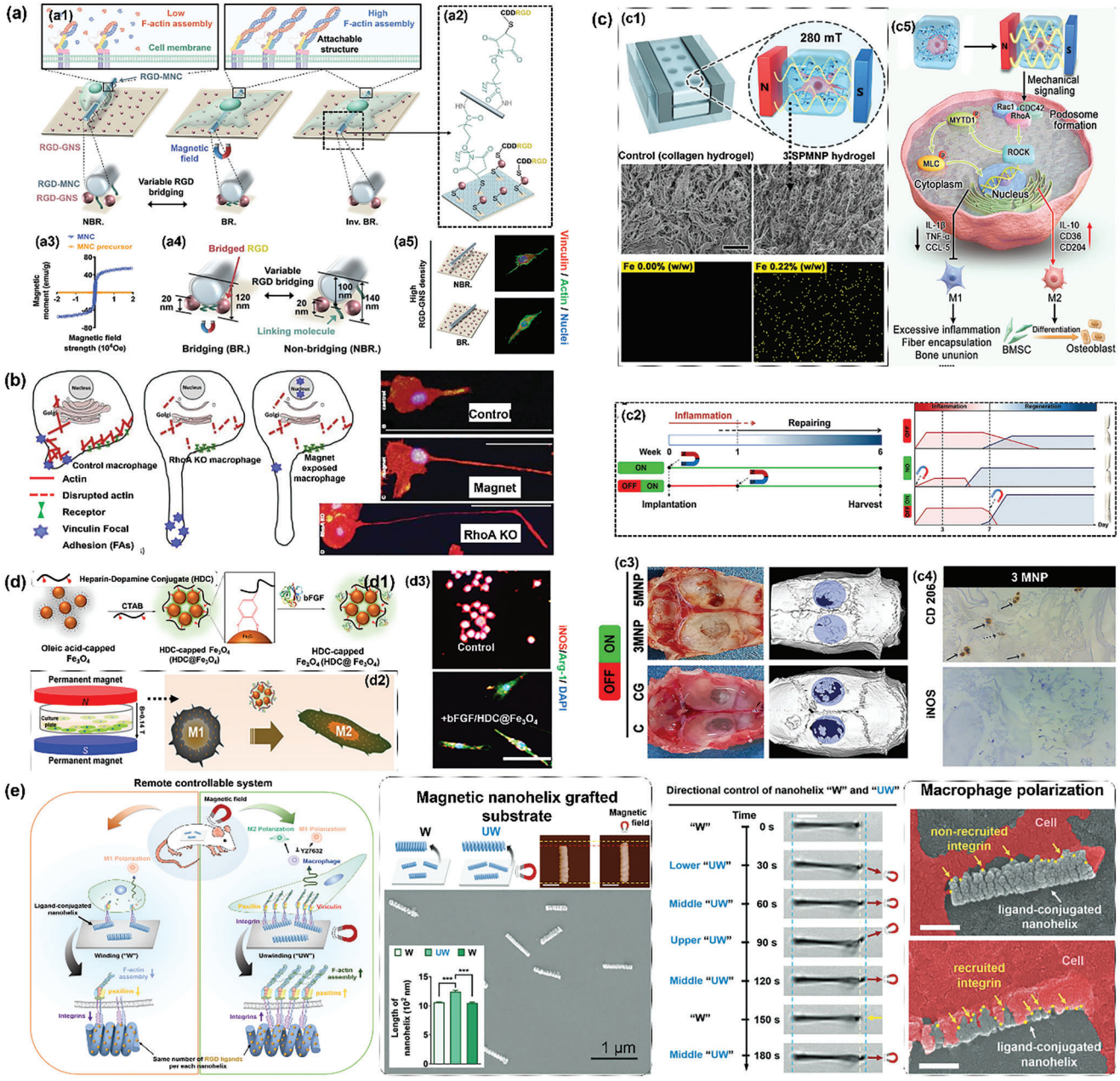

Figure 2. Effect of magnetic field stimuli on macrophage polarization on 2D/3D micro/nanofabricated tissue engineering platforms. a1–a5) Macrophage polarization under magnetic stimuli through in situ ligand bridging platform. (a1) Schematic illustration of the changes in macrophage attachment dynamics to 2D surface through remote control of magnetic nanocylinder (MNC), (a2) The synthesized flexible linker between RGD-coated MNC and gold-nanosphere coated 2D surface, (a3) Vibrating sample magnetometry (VSM) of MNCs and MNC precursors, (a4) magnetically induced movement in the MNC through the flexible linker onto the gold-nanosphere coated 2D surface, (a4) the immunostained confocal images of Vinculin and Actin in the macrophages under the bridged (overlapped MNC/linker/2D surface, under magnetic stimulation) and nonbridged (nonoverlapped MNC/linker/2D surface, without magnetic stimulation) culture conditions. Reproduced with permission.[184] Copyright 2023, Wiley. b) The effect of magnetism and RhoA deletion on actin and actin-related structures in M0 macrophages (upper panel), and the hummingbird phenotype of the magnet exposed and RhoA KO macrophage. Reproduced with permission.[185] Copyright 2018, Elsevier, Cell Press. c) Magnetic stimulation induced on-demand immunomodulation. (c1) The apparatus for magnetic stimulation of 280 mT to superparamagnetic nanoparticle containing hydrogel of collagen nanofibers. (c2) The magnetized ("ON") and nonmagnetized ("OFF") switching of the magnetic stimulation to study the osteo-immunomodulatory process. (c3) μCT images of the cranial bone formation in the presence of magnetic nanoparticles during "ON" condition. (c4) Magnetic nanoparticle-induced M2 macrophage polarization as indicated by the expression of CD206 and iNOS, (c5) Magnetic field induced M1 to M2 macrophage polarization through podosome formation. Reproduced with permission.[186] Copyright 2022, Wiley. d) Magnetic nanoparticle-based platform for the controlled release of growth factor for immunomodulation and skin regeneration. (d1) The synthesis process of the basic fibroblast growth factor (bFGF) loaded iron oxide nanoparticle (bFGF@Fe_3O_4) through the chemical conjugation using heparin–dopamine conjugate. (d2) The bFGF release profile from the developed nanoparticle system. (d3) The in vitro application of magnetic stimuli (140 mT) to cultured macrophages with M2 polarization expressing iNOS and Arg-1 under the

while inhibiting their M1 polarization. According to their findings, it is advantageous to design nanostructured materials with high ligand density and dynamic movement toward the substrate to elicit tissue healing and inflammation-suppressive responses from the implanted materials.[189]

The MF has also been employed intelligently to control the dynamic polarization of macrophages (i.e., M1 through M2). Huang et al. reported the fabrication of a unique immunomodulatory ECM-mimicking hydrogel by grafting superparamagnetic nanoparticles onto collagen nanofibers (Figure 2c).[186] The superparamagnetic nanocomposite hydrogel was manufactured by crosslinking amino-terminated superparamagnetic magnetic nanoparticles (SPMNPs) to collagen fibers with genipin. SPMNPs provided a magnetic response in the hydrogels inside a magnetic chamber comprising two neodymium magnets, producing a uniform static magnetic field of 280 mT (Figure 2c(c1)). By modifying the number of SPMNPs incorporated, the magnetic responsiveness of the hydrogel can be easily optimized toward inflammatory and tissue healing responses (Figure 2c(c2)). A 3% SPMNP and 5% SPMNP induced a sharp transition of M1 to M2 macrophages, as indicated by in vivo bone regeneration and the increased expression of CD206 over iNOS, as shown in Figure 2c(c3,c4). The developed magnetic-responsive hydrogel network efficiently polarized the encapsulated macrophages to the M2 phenotype through the podosome/Rho/ROCK mechanical route in response to a static MF (Figure 2c(c5)). The dynamic regulation of the M1 to M2 transition course preserves the essential role of M1 at the early stage of tissue healing and enhances the healing effect of M2 at the middle/late stages. The in vivo immunomodulatory bone repair was also improved by synchronizing the polarization of macrophages with tissue regeneration. This study effectively orchestrated macrophage polarization from a distance, precisely regulating the early stages of inflammation and subsequent tissue repair. Such nanoplatforms have proven instrumental in integrating various stimuli within a 3D cellular environment. Similar work has been reported by Wu et al., where the authors reported a mussel-inspired heparin-coated magnetic nanoparticle for the sustained release of fibroblast growth factor (Figure 2d).[187] A dopamine–heparin conjugate (HDC) was synthesized and affixed to the surface of Fe_3O_4 MNPs by interacting the dopamine residues of HDC with the nanoparticles (Figure 2d(d1)). Owing to the high binding affinity between basic fibroblast growth factor (bFGF) and heparin, HDC-coated Fe_3O_4 MNPs (HDC@Fe_3O_4) were able to efficiently adsorb bFGF to form bFGF-loaded Fe_3O_4 MNPs (bFGF-HDC@Fe_3O_4). The in vitro study revealed that bFGF-HDC@Fe_3O_4 could effectively control the sustained release of bFGF and modulate in vitro macrophage polarization toward the M2 phenotype indicated by phenotypic changes (Figure 2d(d2)) and higher iNOS expression (Figure 2d(d3)). The wound-healing efficacy of bFGF-HDC@Fe_3O_4 was evaluated using an in vivo full-thickness lesion model. In vivo, data revealed that bFGF-HDC@ Fe_3O_4's induction of M2 polarization and sustained release of bFGF synergistically positively affected wound healing and promoted rapid wound regeneration.

Besides, stimuli-coupled platforms have also shown promising results in controlling other cell types in a coculture environment with macrophages. Vinhas et al. previously reported that magnetic fields modulate the response of human tendon cells (hTDCs) to proinflammatory environments (IL-1-treated-hTDCs) and that magnetically responsive membranes positively affect immune responses. A pulsed electromagnetic field (PEMF) and magnetically responsive membranes were utilized to direct the inflammatory profile of IL-1 treated-hTDCs and macrophages. The results demonstrated that the synergistic effect of PEMF and magnetic membranes supports the applicability of magnetically actuated systems to control inflammatory events and stimulate tendon regeneration.[190]

Bae et al. reported that grafting RGD ligands onto a cobalt sulfate heptahydrate@iron sulfate heptahydrate (CoFe) nanohelical microbots' surface attracts macrophages and induces M2 macrophage polarization.[188] The fabricated CoFe nanohelix-RGD microbots, when unwinded remotely using external MF, showed rapid binding of integrin (≈18.3 integrin binding points/helix) and paxillin (≈17.7 paxillin binding points/helix) owing to the presence of RGD ligand and subsequent M2 polarization. Additionally, when the microbots were actuated in a "winding" mode, the integrin recruitment was attenuated (≈10.7 integrin binding points/helix) and displayed the M1 polarization. The authors further demonstrated that AuNPs-conjugated CoFe nanohelix-RGD could be tracked remotely to study the dynamic macrophage polarization by changing the MF. These results envisioned the role of ligand-conjugated magnetic nanomaterials for real-time tracking and monitoring of macrophage polarization, which will be particularly helpful for elucidating the molecular polarization of macrophages (Figure 2e). **Table 2** summarizes a few more notable micro/nanoplatforms fabricated for macrophage polarization in combination with physical stimulation.

Thus, while an external magnetic field can modulate macrophage polarization, incorporating nanoplatforms offers a multifaceted approach to influencing this polarization. These platforms can elicit diverse responses in macrophage behavior by altering cellular and surface topological characteristics through focal adhesion molecules. Moreover, they can maintain a conducive 3D environment for cell growth during magnetic exposure. Additionally, nanoplatforms can precisely regulate the release of magnetic nanoparticles within hydrogels under

effect of magnetic field and the developed magnetically active nanoparticle system. Reproduced under the terms of the CC-BY 4.0 license.[187] Copyright 2021, American Chemical Society. e, left to right) Schematic illustration of the magnetically controlled winding ("W") and unwinding ("UW") of helical ligand conjugated nanostructure for integrin-mediated macrophage polarization, SEM (lower panel), and AFM images (upper panel) of the magnet responsive nanohelix showing working mechanism and quantitative change in the nanostructure dimension upon external stimulation, time-lapse images of in situ confocal microscopy in real-time for rapid and reversible "W" and "UW" of nanohelix by placing a magnet at various locations (lower, middle, and upper portions) for directional control of the unwinding ("UW") setting or removing the magnet for recovery to the winding ("W") setting within 30 s (scale bar represents 3 μm), paxillin on nanohelix showing increased macrophage adhesion and M2 polarization under magnetic stimulation (scale bar: 300 nm). Reproduced with permission.[188] Copyright 2021, Wiley.

Table 2. A few advanced micro/nanoplatforms fabricated for macrophage polarization in combination with various external physical stimulation.

Stimuli	Micro/nanoplatforms	Stimulation	Macrophage polarization	Mechanism	Refs.
Magnetic field	nHAp/IO@miR-21/124	0.2 T, static	M2	Inhibiting expression of inflammatory markers (TNF-α, iNOS, IL-1β)	[191]
	RGD-SPIONs	124 ± 8 mT, low oscillation (0.1 Hz) High oscillation (2 Hz)	M2 (low oscillation) M1 (high oscillation)	Acute inflammation dominant within 24 h of implantation of scaffold and magnetic field	[74]
	Magnetic manipulation platform (FeNPs, DOX, ICG)	2.4 T min^{-1}, static	M2 to M1 transition	Functionalized MNPs consisting of FeNPs, DOX, and ICG were taken up by macrophages, which then synthesized the MCRs. The proinflammatory M1 phenotype polarized by FeNPs-loaded cell robots.	[169]
	Slidable nanoligand (RGD–PEG–silica-coated IO)	270 mT, static	M2	Magnetic field attracted slidable nanoligand and increased the density of macroscale ligand. This helped assemble adhesion structures in macrophage and facilitate M2 polarization.	[192]
	Fe@Fe_3O_4-DHCA	1 T MRI scanner	No polarization studied	Delivery mediated by macrophages	[193]
	Magnetic liposome (MAN-MNPs@LP)		M2	Mannose-modified magnetic nanoparticles (MANMNPs), loaded on the liposome surface (MAN-MNPs@LP) can accumulate in the lung in response to an SMF and enhance the M2 polarization macrophages through mannose receptor dependent internalization	[194]
	Electrospun Mag-S	5–10 mT, static	M2	Magnetization generated mechanical forces to facilitate M2 polarization, TLR2 and TLR4 expression was downregulated	[195]
Electric field	BaTiO3/Ti6Al4V (BT/Ti) scaffold	Piezoelectric (voltage of 11.5 kV, 30 min)	Promoted M2 polarization	MAPK/JNK signaling pathway was blocked by the piezoelectricity of BT/Ti (poled) scaffolds, and triggered oxidative phosphorylation and ATP production.	[196]

(*Continued*)

Table 2. (Continued)

Stimuli	Micro/nanoplatforms	Stimulation	Macrophage polarization	Mechanism	Refs.
	Pulse capacitive coupling electrical field (PCCEF) (54 mV mm^{-1}, 60 Hz)	Enhanced the M2-type polarization	appropriate pulse width were explored by applying PCCEFs (54 mV mm^{-1}, 60 Hz) of different pulse widths to various cells involved in wound healing and mouse models for 2 h.	[197]	
		Promotes M1 macrophage polarization	The MAPK-p38 pathway is activated by IRE(irreversible electroporation), increasing the release of HMGB1, causes macrophages to express more M1 markers.	[198]	
	P(VDF-TrFE) poly(vinylidene fluoride-trifluoroethylene		Enhanced M2 polarization		[199]
		Pulsed electromagnetic field (PEMF)		FAK signaling	[200]
		Piezoelectric discharge	Enhance the M1 polarization of macrophages	Ultrasound-driven piezoelectric discharge	[201]
Pressure	Electrospun PCL/U4U nanosheets	Pressure, strain range 0–12%	Dominant M1 type	M2 polarization through lower expression of TNF, IL-6, and higher expression of CCR7 and CD206 at 7% strain; M1 polarization through higher expression of TNF and IL-6 at 12% strain	[202]
	Decellularized muscle aponeurosis (D-MA) honeycomb scaffold	Stretching, strain <50%, stress 1.26 kPa	M1 type	M1 polarization through higher expression of iNOS, IL-6, and IL-1β	[203]
Multiple stimuli	NIR + far-red@BCP-GNCs	At power 1.0 and 2.0 W cm^{-2}, 609 nm far-red and 808 nm NIR	M2	M2 polarization (NIR stimulated) and DC maturation (far-red) by releasing IL4 and DXMS (higher expression of BCP-IL4)	[204]

Abbreviations: nHAp: nanohydroxyapatite; IO: iron oxide; miR-21/124: microRNA mi-21-5p and miR-124-3p; RGD: Arg–Gly–Asp sequences; SPIONs: superparamagnetic iron oxide nanoparticles; PP1: peptide; MS: mesoporous silica; IR820: near-infrared fluorescence dye; Fe NPs: ferrous nanoparticles; DOX: doxorubicin; ICG: indocyanine green; MAN: mannose; MNPs: magnetic nanoparticles; LP: liposome; Mag-S: meso-2,3-dimercaptosuccinic acid-coated γ-Fe_2O_3 nanoparticles modified with nHAp and PLA.

controlled MF, facilitating targeted delivery of specific growth factors. Furthermore, leveraging remote control of macrophage polarization holds the potential for directing the behavior of other types of tissue cells.

3.2. Electric Field Coupled Platforms

An EF is another significant stimulus for macrophage polarization on biomimetic platforms. A wound microenvironment is subjected to a severe loss of the body's natural electronic balance, and tissue healing can take longer depending on the severity of the damage. Hence, modern tissue engineering approaches aim to restore the tissue's natural electrical balance to promote healing. Luo et al. reported the fabrication of an electrogenerated dressing (EGD) based on the combination of negative-pressure wound treatment (NPWT, consisting of negative pressure control device and foam dressing) and triboelectric nanogenerator (TENG, a self-powered electrical stimulation system) for skin wound healing.[205] The TENG had two friction layers (aluminum (Al) and poly(tetrafluoroethylene)), two support substrates (poly(ethylene terephthalate), two electrode layers (Cu and Al), a spacer layer, and an encapsulating layer (Kapton). The TENG's electrical output was increased by the friction layers' strip-like surface microstructure, which enhanced the contact area. Support substrates helped separate the TENG friction layer, while the encapsulation layer protected the TENG from exudates, boosting its stability. Periodic dressing deformation caused TENG friction layer contact–separation, which created electron flow and electric potential. The dressing's rectifier changed the built-in TENG's output direction to replicate the endogenous EF's directionality. The annular electrode was put around the wound edge as the anode, and the center electrode was positioned on the wound center as the cathode. In a closed environment, NPWT routinely controlled the pressure change in the dressing, causing the integrated TENG to convert the mechanical energy generated by the shrinkage and relaxation of the dressing into electricity, forming a compensating EF to promote wound healing (**Figure 3**a(a1)). In vitro, data demonstrated that the EGD-generated EF stimulated a robust epithelial electrostatic response and drove macrophages toward a reparative M2 phenotype without causing any harm to cells due to its extremely low current. Subsequent experiments on large animals showed that EDG completely reshaped the wound's EF weakened by NPWT, accelerating proliferation by promoting inflammation/proliferation and wound re-epithelialization by directing epithelial cell migration and proliferation. In addition, EGD accelerates the remodeling period by reconstructing a mature epithelial microstructure and an orderly ECM, thereby enhancing repair quality and decreasing scar formation. The self-powered EF generated by EGD acted as an "electric adjuvant" that flawlessly orchestrated nearly all of the essential phases of wound repair in a noninvasive fashion, thereby revealing its vast clinical potential (Figure 3a(a2)).

The fabricated platform offers distinct advantages over solely relying on electrical stimulation. It effectively balances the endogenous electric field at the wound site and provides a conducive matrix for scarless and rapid re-epithelialization, a feat that may not have been attainable with electric stimulation alone. Diabetic wound healing is more challenging owing to the complexity of the diabetic physiological processes. Electrical stimuli-coupled platforms have also shown promising advancements in such scenarios through macrophage polarization. Dai et al. reported the recreation of the electrical microenvironment for type 2 diabetic hyperglycemic bone regeneration by controlling macrophage polarization through electrical stimulation (Figure 3b).[75] To recreate the electrically conductive bone ECM, the group developed a ferroelectric barium titanate ($BaTiO_3$)/poly(vinylidene fluoridetrifluoroethylene; BTO/P(VDF-TrFE)) nanocomposite membrane using a solution-casting method (Figure 3b(b1)). $BaTiO_3$ nanoparticles were coated with dopamine (Dopa@$BaTiO_3$) and uniformly incorporated on a P(VDF-TrFE) matrix, giving rise to ferroelectric behavior, as confirmed through the characteristic hysteresis loops (Figure 3b(b2)). The developed conductive membrane showed a consistent and continuous stable piezoelectric coefficient of ≈8.19 pC N^{-1}, similar to the native bone. Human monocytic THP-1 macrophages cultured on the unpolarized membrane under normal glucose concentration displayed an inactivated M0 state, and the cells cultured on an unpolarized membrane displayed high glucose-induced M1 polarization. In contrast, the polarized membrane prevented M1 polarization of the cells while promoting M2 polarization through downregulation of the serine/threonine kinase-2/interferon regulatory factor/hypoxia-inducible factor-1α (AKT2-IRF5/HIF-1α) signaling pathway. The attenuation of M1 progression was also noted in the lower expression of iNOS under experimental conditions (Figure 3b(b3)). Electrical stimulation also promoted the osteogenic differentiation of bone marrow-derived mesenchymal stem cells (BM-MSCs). This study lays the groundwork for future investigation and development of electroactive biomaterials, which may have important clinical implications for achieving a favorable immunomodulatory microenvironment for bone regeneration and treatment of inflammatory diseases such as arthritis and atherosclerosis.

Similarly, Park et al. developed a straightforward fabrication method for constructing conductive hydrogels with high electrical conductivity and minimal use of conductive components in various forms for biomedical applications. They specially designed and used graphene-coated agarose microbeads as novel building blocks to produce hydrogel constructs of various geometries and thermally annealed them to induce the formation of conductive graphene networks within the hydrogels. Graphene oxide (GO) and agarose were rearranged into macroporous (honeycomb-like) structures through 60-min thermal annealing at 70 °C. With a modest quantity of GO, the electrical/electrochemical and mechanical properties are significantly enhanced due to the thermal reduction and network formation of GO. The biocompatibility of the developed thermally annealed graphene-channeled agarose hydrogel (TAGAH) was demonstrated through in vitro cell culture and in vivo subcutaneous implantation. TAGAH can be readily shaped into electrically conductive products, including implantable electromyography electrodes, pressure sensors, strain sensors, and 3D tissue scaffolds. With the successful demonstration of its performance and utility, the graphene-channeled conductive hydrogel system will facilitate the facile and versatile fabrication of diverse conductive biomaterials for various biomedical applications.[209] Wang et al. developed a VEGF-loaded micro/nano-3D bionic short nanofiber

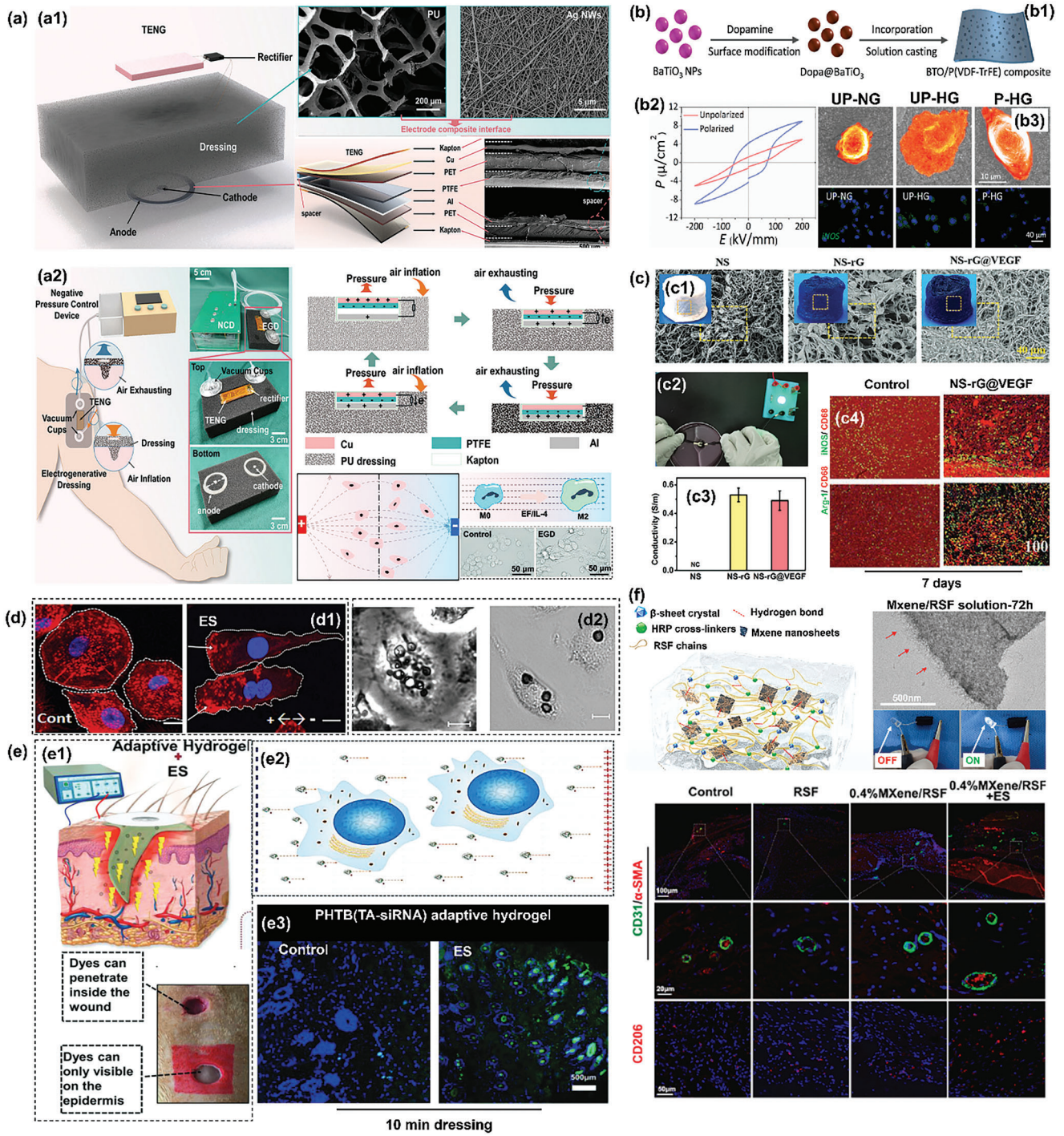

Figure 3. Effect of electric field stimuli on macrophage polarization on 2D/3D micro/nanofabricated tissue engineering platforms. a1,a2) Structural and functional attributes of EGD-NCD conductive system. (a1) Schematic illustration of the developed EGD showing the placements of TENG, rectifier, anode, and the cathode (left), SEM images of the developed platform (polyurethane@silver nanowires) revealing the porous microstructure (right), (a2) Illustration showing the working principle of the EGD-NCD system (left), and schematic illustration of the power generation principle of EGD and HaCaT cell migration and macrophage M2 polarization under electrical stimulation (right). Reproduced with permission.[205] Copyright 2023, Wiley. b1–b3) Fabrication and immunomodulatory effect of BTO/P(VDF-TrFE) composite. (b1) Schematic illustration of the fabrication process of the BTO/P(VDF-TrFE) membrane. (b2) The hysteresis loops of the polarized/unpolarized composite membranes. (b3) SEM images of the electrical stimuli induced changes in the macrophage polarization behavior (upper panel) and the representative immunofluorescence images of iNOS protein (green), cell nuclei (DAPI, blue) (lower panel), UP-NG, unpolarized membrane cultured with normal glucose concentration, UP-HG, unpolarized membrane cultured with high glucose concentration, P-HG, polarized membrane cultured with high glucose concentration. Reproduced under the terms of the CC-BY 4.0 license.[75] Copyright 2021, Elsevier. c1–c4) Short nanofiber sponge composite platform for immunomodulation under electric stimulation, (c1) SEM images of

sponge that could respond to an endogenous electric field and is capable of wound biofluid collection (Figure 3c).[206] The platform fabrication involved electrospinning nanofibers (NFs) consisting of Antheraea pernyi silk fibroin (ApF)/(poly (L-lactic acid-*co*-caprolactone)), followed by NF fragmentation and dispersion in tert-butanol and eventually molding of the homogenized NF into a desired shape and freeze-drying. The fabricated structure was further modified with GO. At a later stage, the coated GO was reduced with the in situ formation of polydopamine (PDA) onto GO from dopamine. The as-fabricated sponge was loaded with VEGF for application (Figure 3c(c1)). The developed platform showed a conductivity within 0.4–0.6 S m^{-1} under dry and wet conditions (Figure 3c(c2,c3)). The conductive platform induced M2 macrophage polarization within seven days of culture, as observed through the reduced expression of iNOS and increased Arg-1 (Figure 3c(c4)). It also showed antibacterial efficiency. This developed platform successfully restored the electric microenvironment to polarize M2 macrophage and activate cellular components through wound collection and the release of essential growth factors. Such micro/nanoplatforms that can recreate the wound's endogenous EF often have fundamentally similar mechanisms. For instance, Hoare et al. studied the influence of electrical fields comparable to the natural electrical environment of the body on human monocyte-derived macrophages.[154] Using live-cell video microscopy, the authors demonstrated that EF as low as 5 mV mm^{-1} influence macrophage movement anodally, culminating at 300 mV mm^{-1} (Figure 3d(d1)). The electrical fields substantially enhanced the phagocytic uptake of various targets by macrophages, including carboxylate beads, apoptotic neutrophils, and the nominal opportunistic pathogen *Candida albicans*, which involved distinct classes of surface receptors (Figure 3d(d2)). These electrical field-induced functional alterations were accompanied by phagocytic receptor clustering, enhanced PI3K and ERK activation, intracellular calcium mobilization, and actin polarization. Some electrical stimuli coupled platforms can facilitate functional gene delivery to promote diabetic wound healing in an electrically stimulated environment. Lei and Fan developed tannic acid (TA)-short interfering RNA (siRNA) (TA-siRNA) injectable nanogels utilizing the self-assembly interaction between TA and siRNA for diabetic wound healing via modulation of macrophage fate (Figure 3e(e1)).[207] The TA-siRNA nanogels contain MMP9 gene-repressing siRNA. To create adaptable conductive PHTB (TA-siRNA) hydrogels, biodegradable TA-siRNA nanogels were crosslinked with poly(vinyl alcohol) (PVA), human-like collagen, TA, and borax. It was estimated that the five catechols and five gallos that make up the terminal subunits of TA could interact with the phosphate backbone of siRNA through hydrogen bonding. The siRNA self-assembled to form nanosized gels because of its small size (20 base pairs). As electrical stimulation generated an electric field between tissues and influenced the movement of charged particles, it was hypothesized that electrical stimulation would facilitate the release of TA-siRNA nanogels from PHTB(TA-siRNA) hydrogels and the consumption of the nanogels by macrophage cells. Though TA-siRNA nanogels interact with macrophage membrane proteins even without an electric field, the number of TA-siRNA nanogels aggregated on the macrophage cell membrane increased, and the cellular uptake rate increased from 35.10% ± 1.12% to 75.40% ± 2.36% in 2 h, indicating that an EF promoted cellular endocytosis. PHTB(TA-siRNA) hydrogels treated with ES exhibited higher green fluorescence than the hydrogels alone. After 20 min of combination treatment, PHTB(TA-siRNA) hydrogels released more siRNA, indicating that ES therapy helps heal wounds (Figure 3e(e2,e3)). MMP9 was strongly expressed in the full-thickness skin defects of diabetic rats in the control group; however, it was considerably reduced in the PHTB(TA-siRNA) hydrogel group and ES therapy-PHTB. These findings show that ES treatment releases and internalizes TA-siRNA nanogels, effectively inhibiting MMP9 mRNA. In addition, ES decreased inflammation and enhanced wound healing by lowering M1 marker expression.

In conjunction with macrophages, an alternative EF on the platform has also been used to control macrophage behavior. Kreller et al. investigated the effect of alternating EF (100 to 150 V m^{-1}) on macrophage polarization and osteoclast differentiation on biomimetic calcium phosphate (BCP)-coated α–β titanium alloy (Ti6Al4V) substrates, a loadbearing implant material, and induced osteoclastic development using growth factors.[210] For 28 days, cells were exposed to directly connected alternating EF (0.7 Vrms, 20 Hz). Indications of a long-term inhibitory effect of ES on osteoclastogenesis and osteoclast activity were suggested by the gradual decrease in the expression rates of genes essential for osteoclast differentiation and activity. An indirect coculture investigation highlighted the effect of ES on intercellular signaling. Except for Carbonic Anhydrase 2 (Car2), genes associated with osteoclast differentiation and activity tended to be downregulated. It was anticipated that ES would specifically activate the calcium signaling pathway by depolarizing the membrane. In tandem with the receptor activator of nuclear factor kappa-β ligand (RANKL) signaling, calcium signaling exhibited a distinct osteoclastogenic potential owing to the robust nuclear factor of activated T cells 1 (NFATc1) induction. Hu et al. discovered that

the nanofibers along with the digital photographs (inset). (c2) The conductivity test of the scaffold through LED test. (c3) The electrical conductivity of the various scaffolds. (c4) Immunostaining images of the polarized macrophages for CD68 and Arg-1. Reproduced with permission.[206] Copyright 2022, Wiley. d1,d2) The effect of electric stimulation on macrophage polarization and migration. (d1) Confocal images of the macrophages showing the alignment of F-actin upon 150 mV mm^{-1} electric field stimulation. (d2) Bright-field image of the macrophages showing the uptake of *C. albicans*, and apoptotic neutrophils after exposure of 150 mV mm^{-1} electric fields. Reproduced with permission.[154] Copyright 2016, Oxford University Press. e) Demonstration of electrically stimulated conductive hydrogels with self-assembled nanogels for delivering siRNAs. (e1) Schematic illustration of the hydrogel fabrication and wound healing study. (e2) Effect of electric fields on cellular adhesion and uptake of the nanogels. (e3) The immunocytochemical images of the wound tissues after the delivery of the TA-siRNA nanogels under electric field stimulation. Reproduced under the terms of the CC-BY 4.0 license.[207] Copyright 2022, Wiley. f) Fabrication and application of an electroactive MXene/RSF hydrogels for immunomodulation-induced bone regeneration. Schematics of the fabricated hydrogel scaffold (top, left), HR-TEM image of the MXene/RSF solution and conductivity test (top, right), and immunostaining images of the Calvaria defect showing the expression of CD31 (green), α-SMA (red), and CD206 (red). Reproduced under the terms of the CC-BY 4.0 license.[208] Copyright 2023, Elsevier.

biocompatible regenerated silk fibroin (RSF) forms nanofibrils with α-sheet structure on MXene nanosheets through straightforward coincubation in aqueous suspensions at physiological temperatures. The developed RSF–MXene hydrogel contained RSF nanofibrils selectively adsorbed at the edge of the MXene nanosheets (Figure 3f). The surface chemistry of the MXene was found to promote the formation of β-sheet structure in the RSF nanofibers. The as-fabricated structure had an electrical conductivity of 4×10^{-4} S cm^{-1}. The fabricated nanoplatforms hydrogel promoted osteogenic differentiation of hBMSCs and M2 macrophage polarization by re-establishing the bone microenvironment, as confirmed through the higher expression of M2 marker Arg-1.[208]

3.3. Pressure and Fluid Shear Stimuli Coupled Platforms

Mechanoimmunology offers yet another novel treatment for inflammatory diseases. Much effort has been made to develop sophisticated platforms capable of facilitating macrophage polarization and tissue regeneration through mechanoimmunological stimuli.

Battiston et al. investigated how monocytes in coculture with human coronary artery smooth muscle cells (VSMCs) regulate the biomolecular phenotype of cells and the ECM of engineered vascular tissue in vitro, cultured on a tubular (3 mm inner diameter) degradable polyurethane scaffold with a combination of nonionic polar, hydrophobic, and ionic chemistry (D-PHI) (**Figure** 4a(a1)). Authors revealed that 10% circumferential strain enhances monocytes/macrophage polarization to M2a macrophage, as evidenced by the higher expression of CD206. Moreover, no M1 polarization of macrophage was identified under the experimental conditions, evidenced by the decrease in the expression of TNF-α and IL-10 (Figure 4a(a2,a3)).[211] The ability of mechanical strain along with M2a macrophages resulted in an increased number of VSMCs, demonstrating the importance of using an appropriate biomechanical environment to understand the activity of VSMCs during tissue remodeling in vivo and in vitro when both cellular (monocytes/macrophages) and biomechanical (circumferential strain) stimuli are present.

Zhang et al. reported a promising biofabrication strategy for immunomodulatory bone regeneration by controlling the osteogenic ability of human umbilical cord-derived mesenchymal stem cells under a compressive mechanical loading environment.[212] A naturally derived hydroxyapatite scaffold was prepared by calcination of cancellous bovine vertebra and further processed into cylindrical (4.5 mm × 10 mm) bone grafts. The cell-scaffold composites were subjected to cyclic mechanical loading using a custom-designed bioreactor system. In the bioreactor chamber, cell-scaffold composites were subjected to a linear wave of cyclic mechanical compression at 1 Hz and a magnitude of 0.06–0.94 MPa for 15 min day^{-1} over 7, 14, or 21 days. Depending on whether the cell-scaffold composites were initially fabricated under mechanical loading or static culture conditions, ECM-based scaffolds facilitated the polarization of macrophages in vitro from a proinflammatory phenotype (M1) to an anti-inflammatory phenotype (M2). In the mechanical loading groups, the mRNA expression levels of IL1B, IL8, human neutrophil activating protein-2, platelet factor-4, and regulated upon activation, normal T cell expressed and presumably secreted were reduced indicating M2 polarization of macrophages (Figure 4b). Applying mechanical loading, in this case, is assumed to alter the ECM architecture, which, in turn, changes the topological environment of the macrophages. The experimental loading conditions that promoted signal transduction favoring M2-specific gene expression might point to the plausible dynamics of the surface receptor expression, the mechanism of which is yet to be explored in detail.

Similarly, Zou et al. developed a multifunctional dressing capable of efficiently absorbing exudate by generating self-micronegative pressure, acting as an antibacterial, and inducing immune regulation for wound healing applications (Figure 4c). A hydrogel–aerogel biphasic gel (HAB-gel) dressing was made of polyvinyl alcohol (PVA) grafted with polyacrylamide (PAM) and biobased polyurethane. The PVA grafted with PAMs produced self-negative pressure to absorb deep exudate by the aerogel phase, providing a comfortable microenvironment for wound healing (Figure 4c(c1)). The hydrogel phase enhanced liquid absorption and retention owing to the porous morphology (Figure 4c(c2,c3)), preventing exudate contamination of the wounds. The incorporation of β-cyclodextrin into constructed polyurethane conferred superior antibacterial properties to HAB-gel materials after loading with polyhexamethylene biguanidine. In addition, the HAB-gel dressing could accelerate the polarization of macrophages into anti-inflammatory M2 macrophages via hydrogen sulfide production, increased IL-10 expression, angiogenesis promotion, and collagen deposition in periwound tissue (Figure 4c(c4)). Overall, this novel strategy for the synergistic treatment of chronic wounds offers a promising method for managing disorders of immunomodulatory tissue regeneration.[76] Li et al. utilized 3D microfluidic tissue culture systems to simulate tumor-associated interstitial flow (3 m s^{-1}) and investigated the effects of interstitial flow on macrophages cultured in 3D collagen I ECM (Figure 4d(d1–d3)). They demonstrated that interstitial flow (IF) promoted M2 polarization of macrophages by elevating the expression of M2 markers Arg-1, TGF-β, CD206, CD163, CD86, and transglutaminase 2 (Figure 4d(d4)). These markers are commonly observed in macrophages associated with malignancies. In addition, they demonstrated that IF facilitates macrophage migration and the ability of macrophages to induce cancer cell invasion, characteristics consistent with those of M2 macrophages associated with tumors. This flow-induced M2-like phenotype depends on integrin/Src-mediated STAT3/6 activation, as revealed by mechanistic analysis. They also discovered that IF directs macrophage migration against the flow direction (upstream). Since IF emanates from the tumor to the surrounding stromal tissues, these findings suggest that IF may encourage tumor progression by promoting macrophage polarization toward the M2 phenotype and recruiting these macrophages from the stromal tissues to the tumor mass.[77]

Macrophages have been polarized under various bioreactor systems through fluid shear stress and the activation of mechanoresponsive receptors and ion channels. Han et al. examined the effects of fluid stress using a perfusion bioreactor on the phenotype and secretory profile of adipose-derived stromal cells (ASCs) cultured on decellularized adipose tissue (DAT) scaffolds in vitro and on the recruitment of host cells following implantation of the preconditioned scaffolds in an athymic-null

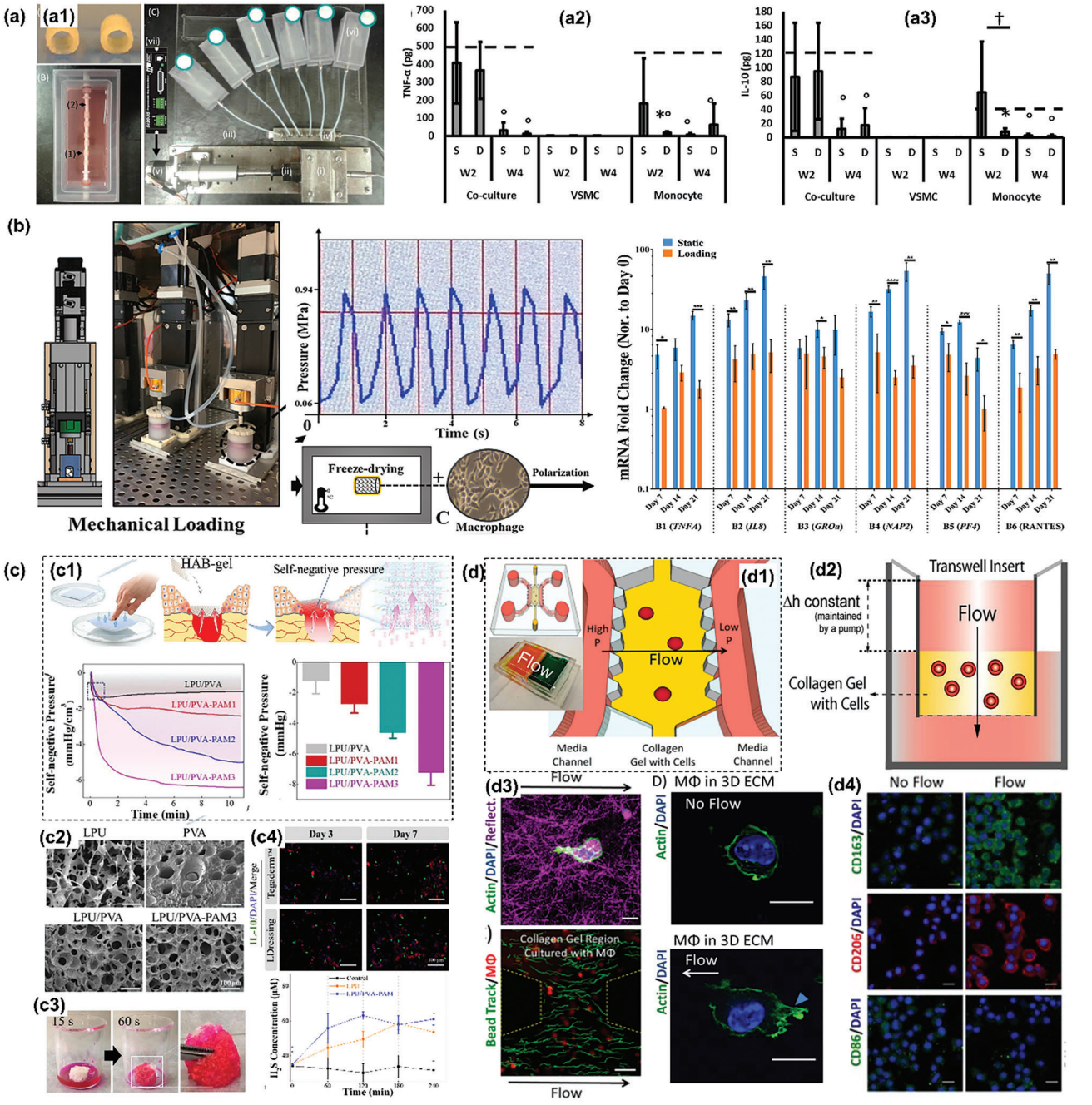

Figure 4. Effect of pressure and fluid shear stimuli on macrophage polarization on 2D/3D micro/nanofabricated tissue engineering platforms. a1–a3) Dynamic mechanical strain induced macrophage polarization on tubular D-PHI scaffolds. (a1) The tubular D-PHI scaffolds (denoted as 1) mounted on distensible silicon tubing (denoted as 2) in a bioreactor setup (comprising of (i) syringe holder, (ii) 50 cc syringe, (iii) bioreactor tray, (iv) manifold, (v) actuator, (vi) syringe filler for gas exchange). (a2) Quantitative assay for the release of TNF-α. (a3) Quantitative assay for the release of IL-10. Reproduced with permission.[211] Copyright 2015, Elsevier. b) Bioreactor setup for the pressure stimulation on cell-scaffold composite and the relative expression of the proinflammatory genes. Reproduced under the terms of the CC-BY 4.0 license.[212] Copyright 2021, Elsevier. (c1–c4) Self-micro-negative pressure generating HAB-gel dressing. Fabrication and application of a hydrogel–aerogel biphasic gel for pressure-induced macrophage polarization and wound healing. (c1) Schematics of the hydrogel fabrication process and negative pressure-induced wound healing application. (c2) FE-SEM image of the fabricated hydrogel scaffolds. (c3) Liquid absorption process of the fabricated hydrogel scaffold. (c4) Immunofluorescence staining images of the wound tissue showing the expression of IL-10 (green) in the presence or absence of the hydrogel scaffold. The representative H_2S generation in the presence of the hydrogels at indicated time points. Reproduced with permission.[76] Copyright 2023, Elsevier. d) Demonstration of interstitial fluid flow-assisted macrophage polarization in vitro. (d1) Schematic illustration of microfluidic chip for macrophage polarization study. (d2) The transwell flow system for evaluating the macrophage polarization. (d3) Immunofluorescence images of the macrophages showing the interaction with collagen fibers and the flow-induced morphological changes. (d4) The immunocytochemical staining of macrophages showing the expression of CD163 (green), CD206 (red), and CD86 (green). Reproduced with permission.[77] Copyright 2018, American Society of Cell Biology.

mouse model. Immunohistochemical analyses revealed that bioreactor culture increased the proportion of ASCs coexpressing iNOS and Arg-1, as well as TNF-α and IL-10 in the peripheral regions of the DAT compared to statically cultured controls. In addition, bioreactor culture altered the expression levels of several immunomodulatory factors in the ASC-seeded DAT. In vivo, testing revealed that cultivating ASCs on the DAT in a perfusion bioreactor before implantation increased the infiltration of host CD31+ endothelial cells and CD26+ cells into the DAT implants but had no effect on the recruitment of CD45+F4/80+CD68+ macrophages. However, in the bioreactor group, a more significant proportion of CD45+ cells expressed the pro-regenerative macrophage marker CD163, which may have contributed to the enhanced remodeling of the scaffolds into host-derived adipose tissue. This study indicates that bioreactor preconditioning can increase the capacity of human ASCs to stimulate regeneration via immunomodulation-mediated mechanisms.[213]

3.4. Photothermal Stimuli Coupled Platforms

Photothermal stimuli-coupled platforms affect macrophages primarily through temperature-induced changes in the nanoplatforms. Zhao et al. synthesized $GdPO_4/CS/Fe_3O_4$ scaffolds for tumor eradication and bone regeneration, integrating Fe_3O_4 nanoparticles and hydrated $GdPO_4$ nanorods into a bioactive chitosan matrix. These multifunctional scaffolds exhibited enhanced NIR absorption and photothermal conversion efficiency, leading to elevated local temperatures under NIR laser irradiation. The scaffolds induced M2 polarization in macrophages through released Gd^{3+} ions, promoting vasculature stabilization and osteogenesis via the BMP-2/Smad/RUNX2 signaling pathway. Consequently, they facilitated photothermal tumor ablation and bone tissue regeneration, potentially offering a treatment avenue for breast cancer bone metastases (**Figure** 5a(a1–a4)). The fabricated scaffolds also triggered the BMP-2/Smad/RUNX2 signaling pathway, aiding cell division, proliferation, and bone tissue regeneration. As a result, the multifunctional $GdPO_4/CS/Fe_3O_4$ scaffolds allow for photothermal ablation of postoperative residual tumors and subsequent bone defect repair, which may turn out to be a potential platform for the treatment of breast cancer bone metastases.[214] Wu et al. engineered an injectable and photocurable hydrogel platform, named AMAD/MP, comprising alginate methacrylate, alginate-graft-dopamine, and PDA-functionalized Ti_3C_2 MXene (MXene@PDA) nanosheets, for NIR-mediated bone regeneration, synergistic immunomodulation, osteogenesis, and bacterial elimination (Figure 5b(b1–b5)). The optimized AMAD/MP hydrogel demonstrated exceptional biocompatibility, osteogenic activity, and immunomodulatory effects in vitro. It effectively balanced macrophage M1/M2 phenotypes, suppressing ROS-induced inflammatory responses. Remarkably, without the addition of exogenous cells, cytokines, or growth factors, this multifunctional hydrogel platform, with moderate thermal stimulation, significantly inhibited local immune responses and promoted new bone formation, facilitated by the enhanced NIR absorbance and photothermal conversion ability conferred by the PDA. The NIR-responsive AMAD/MP hydrogel holds promise for applications in bone tissue engineering and regenerative medicine, showcasing the potential of multifunctional hydrogels with photoactivated thermal stimuli.[215]

To address diabetic wounds through immunomodulation, Yuan et al. developed deferoxamine-loaded mesoporous polydopamine nanoparticles (M@D) by reacting mesoporous PDA nanoparticles (MPDA NPs) with deferoxamine (DFO). They further integrated M@D into an Epigallocatechin-gallate dimer-grafted hyaluronic acid conjugated tyramine-grafted human-like collagen (HTHE)-based hydrogel, formed by enzymatically crosslinking epigallocatechin gallate dimer-grafted hyaluronic acid and tyramine-grafted human-like collagen. Upon NIR laser irradiation, the hydrogel exhibited moderate heat stimulation (≈41 °C) due to the photothermal effect of M@D, releasing DFO in diabetic lesions under acidic conditions. This combined treatment significantly promoted angiogenesis and altered macrophage phenotype, exhibiting outstanding anti-inflammatory properties by M2-polarized macrophages. Compared to a commercial dressing (HeraDerm), the combined treatment accelerated diabetic wound healing in 13 days and facilitated skin tissue regeneration with a more mature skin structure, suggesting a promising therapeutic strategy for diabetic foot ulcer-related wounds (Figure 5c).[78] Similarly, Xu et al. developed a composite hydrogel for immunoregulatory treatment of diabetic wounds, derived from natural polymers. This hydrogel was synthesized by photopolymerizing gelatin methacrylate (GelMA), Bletilla Striata polysaccharide (BSP), and tannic acid/ferric iron complex (TA/Fe^{3+}) in a single step, resulting in adequate mechanical properties due to its chemical and physical crosslinking. Through visible light crosslinking, GelMA, BSP, and TA/Fe^{3+} formed the GBTF hydrogel, exhibiting superior mechanical strength, excellent cytocompatibility, and antioxidant and antibacterial properties. The GBTF hydrogel promoted M2 macrophage polarization via the PI3K/Akt signaling pathway, accelerating diabetic wound healing in vivo by inducing anti-inflammatory and proangiogenic effects. Furthermore, the GBTF hydrogel demonstrated remarkable antibacterial activity under NIR irradiation, suggesting its potential as a photothermal antibacterial wound dressing with promising prospects for the immunological treatment of diabetic wounds.[218] In another approach, Deng et al. developed an F127DA/HAMA-MPDA@SS31 (FH) double-crosslinked hydrogel fortified with SS31-loaded mesoporous polydopamine nanoparticles (MPDA@SS31; M@S NPs) to facilitate the healing of chronic diabetic wounds. This hydrogel exhibited superior biological, injectability, adhesion, and mechanical properties, making it suitable for irregular lesions. Additionally, it possessed antibacterial properties due to the photothermal conversion of MPDA NPs while allowing the sustained release of M@S NPs. Through the controlled release of MPDA NPs and SS31, the FH hydrogel reduced oxidative stress, improved mitochondrial function, regulated macrophage polarization, and promoted wound revascularization, inflammation reduction, and re-epithelialization. In vitro assessments demonstrated its antibacterial activity, enhanced cell viability, ROS scavenging, angiogenesis promotion, and macrophage polarization regulation. Furthermore, in a diabetic wound model, the FH-M@S hydrogel accelerated wound closure by modulating macrophage polarization, enhancing re-epithelialization, collagen deposition, and neovascularization (Figure 5d).[173] Additionally, Zhou et al. introduced a dextran-based hydrogel

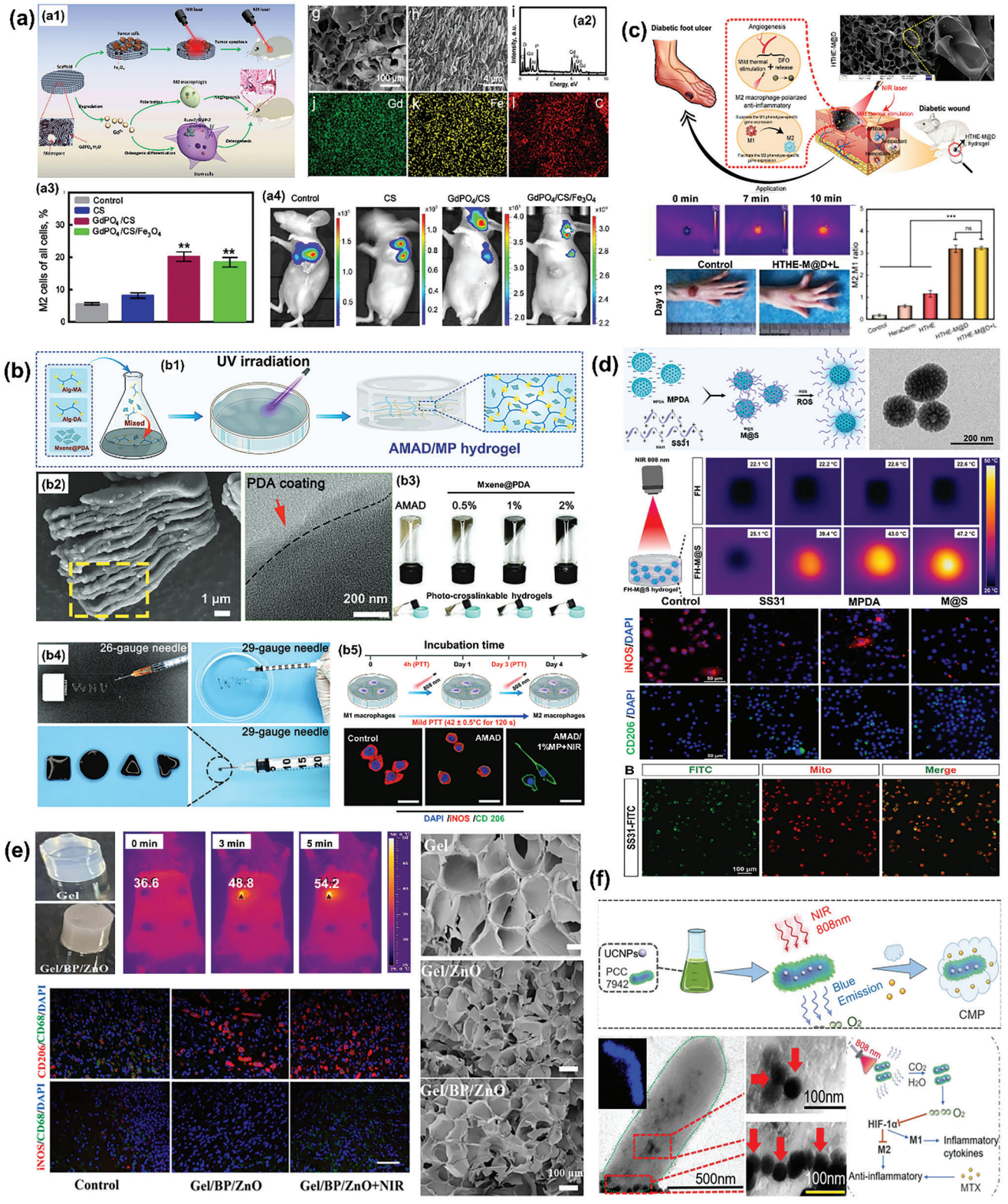

Figure 5. Effect of near-infrared (NIR) stimuli on macrophage polarization on 2D/3D micro/nanofabricated tissue engineering platforms. a) Fabrication and application of a $GdPO_4$ doped 3D printed scaffolds with NIR properties for macrophage polarization and bone regeneration. (a1) Schematic illustration of the study. (a2) FE-SEM and EDS spectra of the CS scaffolds showing the presence of Gd, Fe, and C. (a3) Representative macrophage polarization percentage upon NIR irradiation. (a4) IVIS fluorescence localization of the $GdPO_4$ inside the nude mice after NIR irradiation. Reproduced with permission.[214] Copyright 2020, Elsevier. b) Development of a PDA-capped MXene-based NIR responsive hydrogels for immunomodulation and

bone regeneration. (b1) Schematics of the hydrogel fabrication. (b2) FE-SEM and HR-TEM images of the MXene@PDA nanocomposites. (b3) Digital photographs of the photo-crosslinked MXene@PDA hydrogels. (b4) Injectability and molding ability of the hydrogels. (b5) The immunocytochemical images of the macrophages showing the polarization potential in the presence of the hydrogels upon NIR stimulation. Reproduced with permission.[215] Copyright 2023, Wiley. c) Demonstration of an NIR responsive HTHE-M@D hydrogels for macrophage polarization and diabetic foot ulcer treatment. Reproduced with permission.[78] Copyright 2022, Elsevier. d) Fabrication and application of a double-network hydrogel composing SS31-mesoporous PDA nanoparticles for enhanced photothermal performance and macrophage polarization for diabetic wound treatment. Reproduced under the terms of the CC-BY 4.0 license.[173] Copyright 2023, Elsevier. e) Example of dextran/GelMA/ZnO nanoparticle-based hydrogel platform for macrophage polarization and chronic wound treatment. The fabricated hydrogel scaffold exhibited unique porosity for macrophage adhesion and displayed superior NIR responsiveness for chronic wound treatment. Reproduced with permission.[216] Copyright 2022, Elsevier. f) Fabrication of an NIR responsive and cyanobacteria mimicking nanodevices for modulating macrophage polarization and rheumatoid arthritis therapy. The fabricated nanoplatforms displayed excellent NIR responsive properties and showed M2 macrophage polarization for attenuating the arthritis. Reproduced with permission.[217] Copyright 2021, American Chemical Society.

comprising methacrylated gelatin (GelMA) and oxidized dextran, incorporating nanosheets of black phosphorus (BP) and zinc oxide nanoparticles. When exposed to an 808 nm NIR laser, the hydrogel displayed synergistic antibacterial effects through photothermal action and zinc ion release. The released zinc mitigated macrophage polarization toward the M2 phenotype, known for anti-inflammatory cytokine secretion, thus aiding neovascularization and reducing inflammation. Combined photothermal therapy and immune modulation accelerated wound healing in mouse models with infected full-thickness defect lesions. The Gel/BP/ZnO hydrogel, coupled with NIR treatment, presents a promising strategy for treating chronic ulcers by combining antibacterial and anti-inflammatory properties (Figure 5e).[216]

Furthermore, Guo et al. developed an innovative NIR-controlled cyanobacteria micro/nanodevice for immunotherapy of RA by oxygen-induced lowering of the expression of hypoxia-induced factor-1α (HIF-1α).[217] The cyanobacteria PCC 7942 containing lanthanide upconversion nanoparticles (UCNPs) was utilized to produce O_2 under 700–1000 nm NIR irradiation. The UCNPs could convert the 700–1000 nm NIR into 400–800 nm, facilitating photosynthesis-induced O_2 evolution, M2 macrophage polarization, and drug release (Figure 5f), showcasing the potential of photothermal stimuli-coupled platforms for immunotherapy applications.

Hence, through photothermal stimuli coupled platforms, the desired temperature can be utilized in macrophage polarization through mechanisms such as sustained release of ions, bioactive molecules, and evolution of O_2 in hypoxic wounds, highlighting their efficiency in immunotherapeutic applications.

3.5. Multiple Stimuli Coupled Platforms

Enhancing macrophage response through single stimulation exposure can be further augmented by employing multiple stimulation systems. Utilizing multiple stimuli on platforms to induce macrophage polarization may be necessary to achieve diverse regenerative objectives.[80] Shao et al. designed a novel magnetically responsive mineralized collagen substrate to remotely control macrophages' magnetomechanical stimulation using an external MF and mechanical stretching synergistically. Magnetomechanical stimulation activated M2 macrophage polarization by activating the integrin-related cascade pathway and inhibiting JNK phosphorylation in the MAPK pathway. The optimized inflammatory microenvironment promoted osteogenic differentiation of bone marrow-derived mesenchymal stem cells and osteointegration in vivo. Therefore, this study provides a remote spatiotemporal controllable strategy for promoting osteointegration controlled through mechanical stretching and MF exposure.[219] Further investigation is imperative to elucidate the precise mechanistic underpinnings governing the synergistic effects of these stimuli when applied at the cell–platform interface.

Van Haaften et al. presented an in vitro human model replicating the transient local inflammatory and biomechanical environments that drive scaffold-guided tissue regeneration

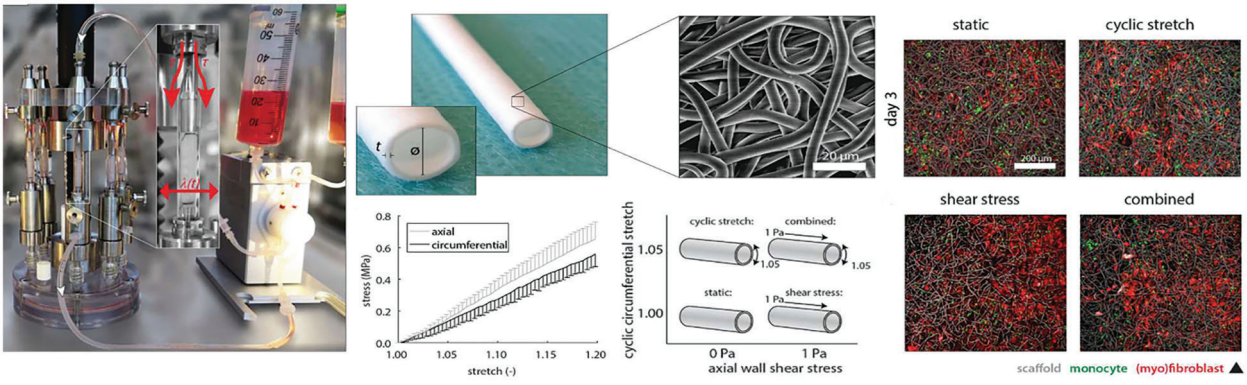

Figure 6. Effect of multiple stimuli on macrophage polarization using 2D/3D micro/nanofabricated platforms; Development of a dynamic bioreactor system coupled with electrospun PCL-PU vascular scaffold for studying the macrophage polarization under cyclic stretching and fluid shear stress. The as-developed platform sustains monocyte viability and promoted the (myo)fibroblast growth after 3 days of incubation. Reproduced under the terms of the CC-BY 4.0 license.[220] Copyright 2020, Wiley.

Table 3. List of a few FDA approved immunomodulatory or physical-stimuli-based tissue engineering devices since 2020–2023.[221]

Platform/device name	Stimuli	Company/developer	Year of approval	Application	Mode of action	Remark
Prospera Spinal Cord Stimulation (SCS) System	Electrical field	Biotronik NRO, Inc.	2023	Implantable spinal cord stimulation system	Electrical signals generated by the implant prevents pain signal from reaching brain	Electrical stimulation can be remotely controlled by using a controller, might have side-effects, and undesirable changes in stimulation may cause tissue damage
Magtrace and Sentimag Magnetic Localization System	Magnetic field	Endomagnetics Ltd.	2022	Assists in the sentinel lymph node biopsies, lumpectomy	Identifies sentinel lymph nodes without exposing patients to radiation	Magtrace (carboxy-dextran coated superparamagnetic iron oxide) flows through lymphatic system to detect cancer; Sentimag identifies cancer location
Selective Cytopheretic Device (SCD)	–	SeaStar Medical	2022	Immuno-modulatory therapy for acute kidney injury	Reduces hyperinflammation on vital organs	Extracorporeal immunomodulatory device, restores immune balance in the body, selectively targets activated neutrophils and monocytes
Sonalleve MR-HIFU-H190003	High intensity ultra sound	Profound Medical Inc., Canada	2020	Treatment of osteoid osteoma	High intensity ultrasound beam induced heat generation and target tissue ablation	Ultrasound energy-induced bone tumor ablation
Vercise PC and Vercise Gevia Deep Brain Stimulation (DBS) system	Low-intensity electrical pulses	Boston Scientific Corporation, Valencia, CA, USA	2020	Treatment for advanced levodopa-responsive Parkinson's disease	Delivers low intensity electrical pulses to brain neurons	Low-intensity electrical pulse mediated reduced tremor and in-voluntary muscle movement
Abbott Infinity DBS Neurostimulation system	Low-intensity electrical pulses	Abbott Medical	2020	Treatment for advanced levodopa-responsive Parkinson's disease	Delivers low intensity electrical pulses to brain neurons	Low-intensity electrical pulse mediated reduced tremor and in-voluntary muscle movement

for immunomodulation-induced muscle regeneration in the scaffold. This model was the basis for coculturing human (myo)fibroblasts and macrophages in a bioreactor platform that decouples cyclic strain and shear stress (**Figure 6**). Employing a biodegradable supramolecular elastomer structure, cyclic stretch initially lowers proinflammatory cytokine release and enhances IL-10 secretion with shear stress. Moreover, cyclic strain stimulates (myo)fibroblast proliferation and the formation of new tissue. When combined with cyclic strain, shear stress synergistically modifies the (myo)fibroblast phenotype. These results indicate that shear stress is a stabilizing factor in cyclic stretch-induced tissue formation and emphasize the distinct functions of hemodynamic loading in the design of resorbable vascular implants.[220]

Thus, integrating various stimuli and nanoplatforms in current and forthcoming research holds significant promise for effectively polarizing macrophages. Manipulating macrophage behavior and polarization to desired states can be achieved by incorporating multiple stimuli, such as electrical, magnetic, and photothermal signals, into advanced nanoplatforms. Magnetic stimulation has demonstrated efficacy in orchestrating topological changes in nanoplatforms, while electric fields can alter cellular polarity, migration, and surface potential through the electrical conductivity of designed platforms. Pressure stimulation coupled platforms can similarly impact the deformation and reformation of the macrophage and matrix interface, thereby modulating macrophage fate. Heat and photothermal therapy also influence exosome secretion, inflammasome formation, and cytokine crosstalk, which are enhanced by integrating nanoplatforms and stimulation. Thus, these considerations should guide the selection of stimuli type and platform.

4. Conclusion and Future Directions

Macrophages are essential for immune response and tissue repair. Treatments target their polarization or capacity to flip between functional phenotypes. Recent advances in micro/nanotechnology have enabled the engineering of sophisticated platforms that accurately regulate macrophage polarization using physical inputs. These systems can revolutionize immunotherapy and tissue regeneration.

Despite the progress in developing stimuli-coupled immunomodulatory platforms, the Food and Drug Administration (FDA) has yet to approve macrophage polarizing platforms. Nevertheless, **Table 3** lists a few immune-modulatory FDA-approved devices using diverse immune cells, encouraging the need to develop macrophage-tunable platforms to achieve clinical success. By engineering microenvironments that promote controlled M1 or M2 polarization, these platforms can enhance antitumor immune responses or suppress excessive inflammation, enhancing healing outcomes. To optimize specificity and efficacy, designing advanced micro/nanoplatforms for stimuli-induced macrophage polarization should prioritize several fundamental principles. These platforms must be designed to guarantee accurate spatiotemporal regulation of stimulus delivery to macrophages, thereby guaranteeing targeted polarization. Integrating numerous stimuli-responsive elements, including responsive polymers or nanoparticles, into the nanoplatforms may facilitate the activation of macrophages in a synergistic fashion. Furthermore, to optimize polarization efficiency, the platforms ought to be engineered to emulate the indigenous microenvironment of macrophages by integrating biomimetic cues, including topographical characteristics and biochemical signals. Additionally, the materials employed in constructing these platforms must possess biocompatibility and biodegradability properties to reduce detrimental effects and promote the seamless integration of tissues. Finally, it is crucial to consider the scalability and reproducibility of manufacturing processes to facilitate the clinical translation and broad application of these sophisticated micro/nanoplatforms designed to induce macrophage polarization in response to stimuli. Future studies should prioritize enhancing the design and production of these advanced nanoplatforms while investigating the underlying molecular pathways contributing to macrophage polarization produced by many stimuli. It is imperative to investigate the potential clinical uses of these groundbreaking methods in immunotherapy, tissue engineering, and regenerative medicine. This is essential for effectively turning laboratory discoveries into meaningful clinical treatments. In summary, combining different stimuli and nanoplatforms shows great potential for improving macrophage polarization approaches and tackling diverse biomedical issues.

Acknowledgements

K.G. and R.L. contributed equally to this work. This study was supported by the "Basic Science Research Program" through the "National Research Foundation of Korea" funded by the "Ministry of Education" (NRF2022R1I1A3063302 and NRF2018R1A6A1A03025582). This work was also supported by Innovative Human Resource Development for Local Intellectualization program through the Institute of Information & Communications Technology Planning & Evaluation (IITP) grant funded by the Korea government (MSIT) (IITP-2024-RS-2023-00260267).

Conflict of Interest

The authors declare no conflict of interest.

Keywords

immunotherapy, macrophages, micro/nanostructures, physical stimuli, tissue regeneration

Received: February 15, 2024
Revised: April 1, 2024
Published online:

[1] A. T. Ruffin, H. Li, L. Vujanovic, D. P. Zandberg, R. L. Ferris, T. C. Bruno, *Nat. Rev. Cancer* **2023**, *23*, 173.
[2] Z. Zhao, C. Li, Y. Zhang, C. Li, Y. Chu, X. Li, P. Liu, H. Chen, Y. Wang, B. Su, Q. Chen, T. Sun, C. Jiang, *Bioact. Mater.* **2023**, *27*, 474.
[3] A. Bascones-Martinez, R. Mattila, R. Gomez-Font, J. H. Meurman, *Med. Oral Patol. Oral Cir. Bucal* **2014**, *19*, 24.
[4] E. Mass, F. Nimmerjahn, K. Kierdorf, A. Schlitzer, *Nat. Rev. Immunol.* **2023**, *23*, 1.
[5] J. Ye, C. Xie, C. Wang, J. Huang, Zi Yin, B. C. Heng, X. Chen, W. Shen, *Bioact. Mater.* **2021**, *6*, 4096.

[6] T. D. Ricketts, N. Prieto-Dominguez, P. S. Gowda, E. Ubil, *Front. Immunol.* **2021**, *12*, 642285.
[7] L. Cassetta, J. W. Pollard, *Nat. Rev. Cancer* **2023**, *23*, 238.
[8] A. Mantovani, A. Sica, M. Locati, *Immunity* **2005**, *23*, 344.
[9] P. J. Murray, *Annu. Rev. Physiol.* **2017**, *79*, 541.
[10] H. Kang, S. H. D. Wong, Q. Pan, G. Li, L. Bian, *Nano Lett.* **2019**, *19*, 1963.
[11] C. Schlundt, H. Fischer, C. H. Bucher, C. Rendenbach, G. N. Duda, K. Schmidt-Bleek, *Acta Biomater.* **2021**, *133*, 46.
[12] S. C. Harwani, *Transl. Res.* **2018**, *191*, 45.
[13] M. Orecchioni, Y. Ghosheh, A. B. Pramod, K. Ley, *Front. Immunol.* **2019**, *10*, 1084.
[14] M. P. Kwesiga, A. A. Gillette, F. Razaviamri, M. E. Plank, A. L. Canull, Z. Alesch, W. He, B. P. Lee, R. J. Guillory, *Bioact. Mater.* **2023**, *23*, 261.
[15] M. Benoit, B. Desnues, J.-L. Mege, *J. Immunol.* **2008**, *181*, 3733.
[16] S. Arora, K. Dev, B. Agarwal, P. Das, M. A. Syed, *Immunobiology* **2018**, *223*, 383.
[17] S. Saranyutanon, S. Acharya, S. K. Deshmukh, M. A. Khan, S. Singh, A. P. Singh, *J. Cell. Physiol.* **2022**, *237*, 1486.
[18] F. Yuan, X. Fu, H. Shi, G. Chen, P. Dong, W. Zhang, *PLoS One* **2014**, *9*, e107063.
[19] S. U. Khan, M. U. Khan, U. D. M. Azhar, I. M. Khan, M. I. Khan, S. Bungau, *Front. Immunol.* **2023**, *14*, 1166487.
[20] M. J. White, R. H. Gomer, *PLoS One* **2015**, *10*, 0138748.
[21] Y. Peng, M. Zhou, H. Yang, R. Qu, Y. Qiu, J. Hao, H. Bi, D. Guo, *Mediators Inflammation* **2023**, *2023*, 8821610.
[22] G. Zizzo, B. A. Hilliard, M. Monestier, P. L. Cohen, *J. Immunol.* **2012**, *189*, 3508.
[23] P. Li, C. Ma, J. Li, S. You, L. Dang, J. Wu, Z. Hao, J. Li, Y. Zhi, L. Chen, S. Sun, *J. Zhejiang Univ., Sci., B* **2022**, *23*, 407.
[24] C. J. Ferrante, G. Pinhal-Enfield, G. Elson, B. N. Cronstein, G. Hasko, S. Outram, S. J. Leibovich, *Inflammation* **2013**, *36*, 921.
[25] Q. Wang, H. Ni, L. Lan, X. Wei, R. Xiang, Y. Wang, *Cell Res.* **2010**, *20*, 701.
[26] C. B. vaz de Paula, M. L. V. de Azevedo, S. Nagashima, A. P. C. Martins, M. A. S. Malaquias, A. F. R. D. S. Miggiolaro, J. da Silva Motta Júnior, G. Avelino, L. A. P. do Carmo, L. B. Carstens, L. de Noronha, *Sci. Rep.* **2020**, *10*, 18689.
[27] S. Gao, J. Zhou, N. Liu, L. Wang, Q. Gao, Y. Wu, Q. Zhao, P. Liu, S. Wang, Y. Liu, N. Guo, Y. Shen, Y. Wu, Z. Yuan, *J. Mol. Cell. Cardiol.* **2015**, *85*, 131.
[28] H.-R. Park, S.-K. Jo, U. Jung, *In Vivo* **2019**, *33*, 1773.
[29] M. Lech, H.-J. Anders, *Biochim. Biophys. Acta, Mol. Basis Dis.* **2013**, *1832*, 989.
[30] Y. Yao, X.-H. Xu, L. Jin, *Front. Immunol.* **2019**, *10*, 792.
[31] Y. Xiong, Z. Lin, P. Bu, T. Yu, Y. Endo, W. Zhou, Y. Sun, F. Cao, G. Dai, Y. Hu, L. Lu, L. Chen, P. Cheng, K. Zha, M.-A. Shahbazi, Q. Feng, B. Mi, G. Liu, *Adv. Mater.* **2023**, *35*, 2212300.
[32] J. M. Lowen, G. C. Bond, K. H. Griffin, N. K. Shimamoto, V. L. Thai, J. K. Leach, *Adv. Healthcare Mater.* **2023**, *12*, 2202239.
[33] Y. Li, J. Zhang, C. Wang, Z. Jiang, K. Lai, Y. Wang, G. Yang, *Acta Biomater.* **2023**, *157*, 108.
[34] H. Xu, Y. Zhu, A. W-T. Hsiao, J. Xu, W. Tong, L. Chang, X. Zhang, Y.-F. Chen, J. Li, W. Chen, Y. Zhang, H. F. Chan, C.-W. Lee, *Biomaterials* **2023**, *294*, 121998.
[35] D. Wen, T. Liang, G. Chen, H. Li, Z. Wang, J. Wang, R. Fu, X. Han, T. Ci, Y. Zhang, P. Abdou, R. Li, L. Bu, G. Dotti, Z. Gu, *Adv. Sci.* **2023**, *10*, 2206001.
[36] X. Wu, Z. Zhong, Y. Li, Y. Wang, Y. Tian, X. Liu, X. Zhang, W. Tao, J. Wang, Y. Du, S. Zhang, *Adv. Funct. Mater.* **2023**, *33*, 2300058.
[37] N. Kartikasari, M. Yamada, J. Watanabe, W. Tiskratok, X. He, Y. Kamano, H. Egusa, *Acta Biomater.* **2022**, *137*, 316.
[38] J. R. Nakkala, Y. Duan, J. Ding, W. Muhammad, D. Zhang, Z. Mao, H. Ouyang, C. Gao, *Acta Biomater.* **2022**, *141*, 24.
[39] P. S. Zieliński, P. K. R. Gudeti, T. Rikmanspoel, M. K. Włodarczyk-Biegun, *Bioact. Mater.* **2023**, *19*, 292.
[40] J. A. Philips, J. D. Ernst, *Annu. Rev. Pathol.: Mech. Dis.* **2012**, *7*, 353.
[41] S. Kadomoto, K. Izumi, A. Mizokami, *Int. J. Mol. Sci.* **2021**, *23*, 144.
[42] F. O. Martinez, S. Gordon, M. Locati, A. Mantovani, *J. Immunol.* **2006**, *177*, 7303.
[43] D. M. Mosser, *J. Leukoc. Biol.* **2003**, *73*, 209.
[44] D. K. Dalton, S. Pitts-Meek, S. Keshav, I. S. Figari, A. Bradley, T. A. Stewart, *Science* **1993**, *259*, 1739.
[45] S. Bashir, Y. Sharma, A. Elahi, F. Khan, *Inflammation Res.* **2016**, *65*, 1.
[46] M. H. M. Barros, F. Hauck, J. H. Dreyer, B. Kempkes, G. Niedobitek, *PLoS One* **2013**, *8*, 80908.
[47] S. Gordon, F. O. Martinez, *Immunity* **2010**, *32*, 593.
[48] M. Munder, *Br. J. Pharmacol.* **2009**, *158*, 638.
[49] J. M. Dzik, *Front. Immunol.* **2014**, *5*, 544.
[50] G. Mondanelli, R. Bianchi, M. T. Pallotta, C. Orabona, E. Albini, A. Iacono, M. L. Belladonna, C. Vacca, F. Fallarino, A. Macchiarulo, S. Ugel, V. Bronte, F. Gevi, L. Zolla, A. Verhaar, M. Peppelenbosch, E. M. C. Mazza, S. Bicciato, Y. Laouar, L. Santambrogio, P. Puccetti, C. Volpi, U. Grohmann, *Immunity* **2017**, *46*, 233.
[51] O. Butovsky, Y. Ziv, A. Schwartz, G. Landa, A. E. Talpalar, S. Pluchino, G. Martino, M. Schwartz, *Mol. Cell. Neurosci.* **2006**, *31*, 149.
[52] A. M. Nikolakopoulou, R. Dutta, Z. Chen, R. H. Miller, B. D. Trapp, *Proc. Natl. Acad. Sci. USA* **2013**, *110*, 8714.
[53] J. G. Tidball, S. A. Villalta, *Am. J. Physiol.: Regul., Integr. Comp. Physiol.* **2010**, *298*, R1173.
[54] D. A. Chistiakov, Y. V. Bobryshev, N. G. Nikiforov, N. V. Elizova, I. A. Sobenin, A. N. Orekhov, *Int. J. Cardiol.* **2015**, *184*, 436.
[55] F. O. Martinez, A. Sica, A. Mantovani, M. Locati, *Front. Biosci.-Landmark* **2008**, *13*, 453.
[56] B. Vidal, A. L. Serrano, M. Tjwa, M. Suelves, E. Ardite, R. De Mori, B. Baeza-Raja, M. M. de Lagrán, P. Lafuste, V. Ruiz-Bonilla, M. Jardí, R. Gherardi, C. Christov, M. Dierssen, P. Carmeliet, J. L. Degen, M. Dewerchin, P. Muñoz-Cánoves, *Genes Dev.* **2008**, *22*, 1747.
[57] W. Foster, Y. Li, A. Usas, G. Somogyi, J. Huard, *J. Orthop. Res.* **2003**, *21*, 798.
[58] F. O. Martinez, L. Helming, S. Gordon, *Annu. Rev. Immunol.* **2009**, *27*, 451.
[59] A. Shapouri-Moghaddam, S. Mohammadian, H. Vazini, M. Taghadosi, S.-A. Esmaeili, F. Mardani, B. Seifi, A. Mohammadi, J. T. Afshari, A. Sahebkar, *J. Cell. Physiol.* **2018**, *233*, 6425.
[60] D. A. Chistiakov, Y. V. Bobryshev, A. N. Orekhov, *J. Cell. Mol. Med.* **2015**, *19*, 1163.
[61] G. Haskó, P. Pacher, E. A. Deitch, E. S. Vizi, *Pharmacol. Ther.* **2007**, *113*, 264.
[62] A. Sica, A. Mantovani, *J. Clin. Invest.* **2012**, *122*, 787.
[63] J. W. Pollard, *Nat. Rev. Cancer* **2004**, *4*, 71.
[64] B. S. Calin, I. A. Paun, *Int. J. Mol. Sci.* **2022**, *23*, 14270.
[65] J. E. Park, S. Won, W. Cho, J. G. Kim, S. Jhang, J. G. Lee, J. J. Wie, *J. Polym. Sci.* **2021**, *59*, 1491.
[66] L. Wu, Y. Xu, K. Xi, Y. Gu, J. Tang, T. Xin, H. Yang, L. Wang, W. Cui, L. Chen, *Chem. Eng. J.* **2022**, *439*, 135692.
[67] Z. Zhou, J. Zhang, X. He, X. Chen, L. Dong, J. Lin, H. Wang, W. Weng, K. Cheng, *ACS Biomater. Sci. Eng.* **2023**, *9*, 2524.
[68] Y. Gao, W. Dai, Z. Ouyang, M. Shen, X. Shi, *Biomacromolecules* **2023**, *24*, 886.
[69] M. Vassey, L. Ma, L. Kämmerling, C. Mbadugha, G F. Trindade, G. P. Figueredo, F. Pappalardo, J. Hutchinson, R. Markus, S. Rajani, Q. Hu, D. A. Winkler, D. J. Irvine, R. Hague, A. M. Ghaemmaghami, R. Wildman, M. R. Alexander, *Matter* **2023**, *6*, 887.

[70] R. Sridharan, A. R. Cameron, D. J. Kelly, C. J. Kearney, F. J. O'Brien, *Mater. Today* **2015**, *18*, 313.
[71] N. Jain, J. Moeller, V. Vogel, *Annu. Rev. Biomed. Eng.* **2019**, *21*, 267.
[72] C. Kerneur, C. E. Cano, *Front. Immunol.* **2022**, *13*, 1026954.
[73] N. Wang, H. Liang, K. Zen, *Front. Immunol.* **2014**, *5*, 614.
[74] H. Kang, S. Kim, D. S. H. Wong, H. J. Jung, S. Lin, K. Zou, R. Li, G. Li, V P. Dravid, L. Bian, *Nano Lett.* **2017**, *17*, 6415.
[75] X. Dai, B. C. Heng, Y. Bai, F. You, X. Sun, Y. Li, Z. Tang, M. Xu, X. Zhang, X. Deng, *Bioact. Mater.* **2021**, *6*, 2029.
[76] F. Zou, Y. Wang, T. Tang, Y. Zheng, Y. Xie, S. Zhu, H. Yang, H. Meng, X. Liu, J. Yang, *Chem. Eng. J.* **2023**, *451*, 138952.
[77] R. Li, J. C. Serrano, H. Xing, T. A. Lee, H. Azizgolshani, M. Zaman, R. D. Kamm, *Mol. Biol. Cell* **2018**, *29*, 1927.
[78] Y. Yuan, D. Fan, S. Shen, X. Ma, *Chem. Eng. J.* **2022**, *433*, 133859.
[79] X. Deng, H. Liang, W. Yang, Z. Shao, *J. Photochem. Photobiol., B* **2020**, *208*, 111913.
[80] A. D. Schoenenberger, H. Tempfer, C. Lehner, J. Egloff, M. Mauracher, A. Bird, J. Widmer, K. Maniura-Weber, S. F. Fucentese, A. Traweger, U. Silvan, J. G. Snedeker, *Biomaterials* **2020**, *249*, 120034.
[81] P. Li, Z. Hao, J. Wu, D. Fan, S. Sun, *Front. Immunol.* **2021**, *12*, 700009.
[82] X. Feng, Y. Ji, C. Zhang, T. Jin, J. Li, J. Guo, *Exp. Dermatol.* **2023**, *32*, 403.
[83] F. Bellora, R. Castriconi, A. Dondero, G. Reggiardo, L. Moretta, A. Mantovani, A. Moretta, C. Bottino, *Proc. Natl. Acad. Sci. USA* **2010**, *107*, 21659.
[84] C. Chen, J. Cao, Y. Gao, X. Xie, Z. Zhao, Q. Yuan, et al., *Genes Dis.* **2024**, *11*, 539.
[85] M. L. Sowers, H. Tang, V. K. Singh, A. Khan, A. Mishra, B. I. Restrepo, et al., *J. Biol. Chem.* **2022**, *298*, 102418.
[86] M. Portou, D. Baker, D. Abraham, J. Tsui, *Vasc. Pharmacol.* **2015**, *71*, 31.
[87] S. Tartey, O. Takeuchi, *Int. Rev. Immunol.* **2017**, *36*, 57.
[88] Z. Pang, R. D. Junkins, R. Raudonis, A. J. MacNeil, C. McCormick, Z. Cheng, T.-J. Lin, *PLoS One* **2018**, *13*, 0197491.
[89] K. K. Asanka Sanjeewa, T. U. Jayawardena, H.-S. Kim, S.-Y. Kim, I. P. Shanura Fernando, L. Wang, D. T. U. Abetunga, W.-S. Kim, D.-S. Lee, Y.-J. Jeon, *Carbohydr. Polym.* **2019**, *224*, 115195.
[90] S. Udayan, L. F. Buttó, V. Rossini, J. Velmurugan, M. Martinez-Lopez, D. Sancho, S. Melgar, P. W. O'Toole, K. Nally, *Sci. Rep.* **2021**, *11*, 5896.
[91] Z. Xu, X. Hao, M. Li, H. Luo, *Int. J. Mol. Sci.* **2022**, *23*, 9742.
[92] A.-Y. Hong, S.-J. Lee, K. B. Lee, J.-W. Shin, E. M. Jeong, I.-G. Kim, *Int. J. Mol. Sci.* **2022**, *23*, 2709.
[93] H I. Muendlein, W M. Connolly, Z. Magri, D. Jetton, I. Smirnova, A. Degterev, S. Balachandran, A. Poltorak, *Proc. Natl. Acad. Sci. USA* **2022**, *119*, 2113872119.
[94] R. Su, L. Cai, P. Xiong, Z. Liu, S. Chen, X. Liu, R. Lin, Z. Lei, D. Tian, M. Su, *J. Inflammation Res.* **2022**, *15*, 1437.
[95] A. Baradaran, Z. Asadzadeh, N. Hemmat, A. Baghbanzadeh, M. A. Shadbad, N. Khosravi, et al., *Biomed. Pharmacother.* **2022**, *146*, 112588.
[96] K. M. Sheu, A. Hoffmann, *Annu. Rev. Immunol.* **2022**, *40*, 295.
[97] M. Lopez-Yrigoyen, L. Cassetta, J. W. Pollard, *Ann. N. Y. Acad. Sci.* **2021**, *1499*, 18.
[98] M. Shah, G.-Y Kim, A. Achek, E.-Y. Cho, W.-Y. Baek, Y. S. Choi, W. H. Lee, D.-J. Kim, S. H. Lee, W. Kim, S. S. Kim, J. Y. Cheong, C.-H. Suh, S. Choi, *Biomaterials* **2020**, *245*, 119974.
[99] K. M.-C. Lee, A. A. Achuthan, D. P. De Souza, T. J. Lupancu, K. J. Binger, M. K. Lee, et al., *Cell Rep.* **2022**, *39*, 110719.
[100] R. P. De Maeyer, E. S. Chambers, *Immunol. Lett.* **2021**, *230*, 1.
[101] M. Gracia-Hernandez, E. M. Sotomayor, A. Villagra, *Front. Pharmacol.* **2020**, *11*, 577571.
[102] X. Hu, J. Li, M. Fu, X. Zhao, W. Wang, *Signal Transduction Targeted Ther.* **2021**, *6*, 402.
[103] Y. Liu, L. Wang, S. Li, T. Zhang, C. Chen, J. Hu, D. Sun, H. Lu, *J. Orthop. Translat.* **2022**, *37*, 78.
[104] T. Xia, M. Zhang, W. Lei, R. Yang, S. Fu, Z. Fan, Y. Yang, T. Zhang, *Front. Immunol.* **2023**, *14*, 1160719.
[105] I. Malyshev, Y. Malyshev, *Biomed Res. Int.* **2015**, *2015*, 1.
[106] L. B. Ivashkiv, *Nat. Rev. Immunol.* **2018**, *18*, 545.
[107] D. M. Calcagno, R. P. Ng, A. Toomu, C. Zhang, K. Huang, A. D. Aguirre, R. Weissleder, L. B. Daniels, Z. Fu, K. R. King, *Sci. Immunol.* **2020**, *5*, 1974.
[108] S. Lu, D. Li, L. Xi, R. Calderone, *Microb. Pathog.* **2019**, *134*, 103594.
[109] F. Wang, S. Zhang, R. Jeon, I. Vuckovic, X. Jiang, A. Lerman, C D. Folmes, P D. Dzeja, J. Herrmann, *EBioMedicine* **2018**, *30*, 303.
[110] S. Xia, Y. Tao, L. Cui, Y. Yu, S. Xu, *J. Immunol. Res.* **2019**, *2019*, 1.
[111] D. A. Chistiakov, V. A. Myasoedova, V. V. Revin, A. N. Orekhov, Y. V. Bobryshev, *Immunobiology* **2018**, *223*, 101.
[112] J. Liu, H. Wang, L. Zhang, X. Li, X. Ding, G. Ding, F. Wei, *J. Leukocyte Biol.* **2022**, *111*, 1185.
[113] Y. Miao, L. He, X. Qi, X. Lin, *Front. Mol. Biosci.* **2020**, *7*, 603817.
[114] Y. Okamoto, K. Kitakaze, Y. Takenouchi, S. Yamamoto, H. Ishimaru, K. Tsuboi, *Cell. Signalling* **2021**, *88*, 110156.
[115] Y. Li, Q. Sheng, C. Zhang, C. Han, H. Bai, P. Lai, Y. Fan, Y. Ding, X. Dou, *Int. Immunopharmacol.* **2021**, *91*, 107266.
[116] Z. J. Bernstein, A. Shenoy, A. Chen, N. M. Heller, J. B. Spangler, *Immunol. Rev.* **2023**, *320*, 29.
[117] L. Lis-López, C. Bauset, M. Seco-Cervera, J. Cosín-Roger, *Biomedicines* **2021**, *9*, 1747.
[118] C. E. Witherel, K. Sao, B. K. Brisson, B. Han, S. W. Volk, R. J. Petrie, L. Han, K. L. Spiller, *Biomaterials* **2021**, *269*, 120667.
[119] Y. Jian, X. Zhou, W. Shan, C. Chen, W. Ge, J. Cui, W. Yi, Y. Sun, *Cell Commun. Signaling* **2023**, *21*, 1.
[120] M.-Z. Zhang, X. Wang, Y. Wang, A. Niu, S. Wang, C. Zou, R. C. Harris, *Kidney Int.* **2017**, *91*, 375.
[121] A. Mantovani, S. K. Biswas, M. R. Galdiero, A. Sica, M. Locati, *J. Pathol.* **2013**, *229*, 176.
[122] W.-C. Yang, Y.-S. Hwang, Y.-Y. Chen, C.-L. Liu, C.-N. Shen, W.-H. Hong, S.-M. Lo, C.-R. Shen, *Front. Immunol.* **2017**, *8*, 1508.
[123] A. J. Boutilier, S. F. Elsawa, *Int. J. Mol. Sci.* **2021**, *22*, 6995.
[124] T. Liu, L. Zhang, D. Joo, S.-C. Sun, *Signal Transduction Targeted Ther.* **2017**, *2*, 1.
[125] M. G. Dorrington, I. D. Fraser, *Front. Immunol.* **2019**, *10*, 705.
[126] L. Barnabei, E. Laplantine, W. Mbongo, F. Rieux-Laucat, R. Weil, *Front. Immunol.* **2021**, *12*, 716469.
[127] S. Fakhri, S. Z. Moradi, A. Yarmohammadi, F. Narimani, C. E. Wallace, A. Bishayee, *Front. Oncol.* **2022**, *12*, 834072.
[128] C. Gasparini, M. Feldmann, *Curr. Pharm. Des.* **2012**, *18*, 5735.
[129] M. Hernandez-Quiles, M. F. Broekema, E. Kalkhoven, *Front. Endocrinol.* **2021**, *12*, 624112.
[130] Y. Shu, M. Qin, Y. Song, Q. Tang, Y. Huang, P. Shen, Y. Lu, *Immunology* **2020**, *160*, 345.
[131] C. Ciavarella, I. Motta, S. Valente, G. Pasquinelli, *Molecules* **2020**, *25*, 2076.
[132] A. K. Reka, M. T. Goswami, R. Krishnapuram, T. J. Standiford, V. G. Keshamouni, *Lung Cancer* **2011**, *72*, 154.
[133] V. L. Nelson, H. C. Nguyen, J. C. Garcìa-Cañaveras, E. R. Briggs, W. Y. Ho, J. R. DiSpirito, et al., *Genes Dev.* **2018**, *32*, 1035.
[134] J. L. Wilson, H. K. Mayr, T. Weichhart, *Front. Immunol.* **2019**, *10*, 2265.
[135] D. Montaigne, L. Butruille, B. Staels, *Nat. Rev. Cardiol.* **2021**, *18*, 809.
[136] Y. Wang, M. Zhao, S. Liu, J. Guo, Y. Lu, J. Cheng, J. Liu, *Cell Death Dis.* **2020**, *11*, 924.
[137] B. Daniel, G. Nagy, Z. Czimmerer, A. Horvath, D. W. Hammers, I. Cuaranta-Monroy, S. Poliska, P. Tzerpos, Z. Kolostyak, T. T. Hays, A. Patsalos, R. Houtman, S. Sauer, J. Francois-Deleuze, F. Rastinejad, B. L. Balint, H. L. Sweeney, L. Nagy, *Immunity* **2018**, *49*, 615.

[138] Y. Wang, A. H. van Boxel-Dezaire, H. Cheon, J. Yang, G. R. Stark, *Proc. Natl. Acad. Sci. USA* **2013**, *110*, 16975.
[139] T. Mori, T. Miyamoto, H. Yoshida, M. Asakawa, M. Kawasumi, T. Kobayashi, H. Morioka, K. Chiba, Y. Toyama, A. Yoshimura, *Int. Immunol.* **2011**, *23*, 701.
[140] Z. Duan, Y. Luo, *Signal Transduction Targeted Ther.* **2021**, *6*, 127.
[141] J. J. Balic, H. Albargy, K. Luu, F. J. Kirby, W. S. N. Jayasekara, F. Mansell, D. J. Garama, D. De Nardo, N. Baschuk, C. Louis, F. Humphries, K. Fitzgerald, E. Latz, D. J. Gough, A. Mansell, *Nat. Commun.* **2020**, *11*, 3816.
[142] S. V. Aguilar, O. Aguilar, R. Allan, V. Angeli, M. N. Artyomov, N. Asinovski, et al., *Nat. Immunol.* **2020**, *21*, 700.
[143] C. Vergallo, L. Dini, Z. Szamosvölgyi, B. A. Tenuzzo, E. Carata, E. Panzarini, J. F. László, *PLoS One* **2013**, *8*, 72374.
[144] S. Kim, B. Lee, J. Moon, M. Ahn, H. Lee, *IEEE Trans. Magn.* **2023**, *59*, 1.
[145] C. L. Ross, B. S. Harrison, *Electromagn. Biol. Med.* **2013**, *32*, 59.
[146] S. J. Kim, Y. W Jang, K. E. Hyung, D. K. Lee, K. H. Hyun, S. H. Jeong, K. H. Min, W. Kang, J. H. Jeong, S.-Y. Park, K. W. Hwang, *Bioelectromagnetics* **2017**, *38*, 374.
[147] J. Frahm, M. Lantow, M. Lupke, D. G. Weiss, M. Simkó, *J. Cell. Biochem.* **2006**, *99*, 168.
[148] E. G. Novoselova, V. V. Novikov, S. M. Lunin, O. V. Glushkova, T. V. Novoselova, S. B. Parfenyuk, S. V. Novoselov, M. O. Khrenov, E. E. Fesenko, *Electromagn. Biol. Med.* **2019**, *38*, 74.
[149] H. Lei, Y. Pan, R. Wu, Y. Lv, *Front. Immunol.* **2020**, *11*, 582772.
[150] M. R. Cho, H. S. Thatte, R. C. Lee, D. E. Golan, *Ann. Biomed. Eng.* **2000**, *28*, 234.
[151] K. He, S. Jia, Y. Lou, P. Liu, L. X. Xu, *Cell Death Dis.* **2019**, *10*, 216.
[152] J. Feehan, N. Tripodi, S. Fraser, K. Mikkelsen, A. Thewlis, D. Kiatos, M. Husaric, V. Apostolopoulos, *J. Biophotonics* **2020**, *13*, 201960177.
[153] C. Chen, X. Bai, Y. Ding, I.-S. Lee, *Biomater. Res.* **2019**, *23*, 1.
[154] J. I. Hoare, A. M. Rajnicek, C. D. McCaig, R. N. Barker, H. M. Wilson, *J. Leukocyte Biol.* **2016**, *99*, 1141.
[155] C.-T. Lee, L. Zhong, T. A. Mace, E. A. Repasky, *PLoS One* **2012**, *7*, 30077.
[156] Di Xu, Z. Liu, M.-X. Liang, W.-Q. Chen, Y.-J. Fei, S.-J. Yang, Y. Wu, W. Zhang, J.-H. Tang, *Discover Oncol.* **2023**, *14*, 81.
[157] B. Li, F. Liu, J. Ye, X. Cai, R. Qian, K. Zhang, Y. Zheng, S. Wu, Y. Han, *Small* **2022**, *18*, 2202691.
[158] P. Liu, X. Liu, L. Zhang, G. Yan, H. Zhang, D. Xu, Y. Wu, G. Zhang, P. Wang, Q. Zeng, X. Wang, *Biochem. Pharmacol.* **2023**, *208*, 115403.
[159] L. Wang, W. Zhang, R. Cen, C. Yue, T. Xiao, Y. Deng, L. Li, K. Sun, X. Lei, *Lasers Surg. Med.* **2022**, *54*, 1309.
[160] K. Woo, S. Y. Park, A. Padalhin, H. S. Ryu, C. D. Abueva, *J. Photochem. Photobiol., B* **2023**, *246*, 112770.
[161] S. Adams, L. M. Wuescher, R. Worth, E. Yildirim-Ayan, *Ann. Biomed. Eng.* **2019**, *47*, 2213.
[162] J. Iqbal, M. Zaidi, *Biochem. Biophys. Res. Commun.* **2005**, *328*, 751.
[163] B. Wang, M. Kasper, B. Laffer, G. Meyer zu Hörste, S. Wasmuth, M. Busch, T. V. Jalilvand, S. Thanos, A. Heiligenhaus, D. Bauer, C. Heinz, *Front. Immunol.* **2020**, *11*, 573955.
[164] K. Maruyama, E. Nemoto, S. Yamada, *Inflammation Regener.* **2019**, *39*, 1.
[165] C. Li, C. Li, Z. Ma, H. Chen, H. Ruan, L. Deng, J. Wang, W. Cui, *Bioact. Mater.* **2023**, *19*, 474.
[166] S. D. Dutta, K. Ganguly, T. V. Patil, A. Randhawa, K.-T. Lim, *Bioact. Mater.* **2023**, *28*, 284.
[167] D. Kosoff, J. Yu, V. Suresh, D. J. Beebe, J. M. Lang, *Lab Chip* **2018**, *18*, 3011.
[168] B. M. Tiemeijer, M. W. D. Sweep, J. J. F. Sleeboom, K. J. Steps, J. F. van Sprang, P. De Almeida, R. Hammink, P. H. J. Kouwer, A. I. P. M. Smits, J. Tel, *Front. Bioeng. Biotechnol.* **2021**, *9*, 715408.
[169] Y. Dai, X. Bai, L. Jia, H. Sun, Y. Feng, L. Wang, C. Zhang, Y. Chen, Y. Ji, D. Zhang, H. Chen, L. Feng, *Small* **2021**, *17*, 2103986.
[170] X. Song, W. Fu, U. K. Cheang, *IScience* **2022**, *25*, 1.
[171] K. Garg, N. A. Pullen, C. A. Oskeritzian, J. J. Ryan, G. L. Bowlin, *Biomaterials* **2013**, *34*, 4439.
[172] Y. Wang, D. Yao, L. Li, Z. Qian, W. He, R. Ding, et al., *ACS Biomater. Sci. Eng.* **2020**, *6*, 3502.
[173] Q.-S. Deng, Y. Gao, B.-Y. Rui, X.-R. Li, P.-L. Liu, Z.-Y. Han, Z.-Y. Wei, C.-R. Zhang, F. Wang, H. Dawes, T.-H. Zhu, S.-C. Tao, S.-C. Guo, *Bioact. Mater.* **2023**, *27*, 409.
[174] D. Wang, M. Zhang, G. Qiu, C. Rong, X. Zhu, G. Qin, et al., *ACS Nano* **2023**, *17*, 5503.
[175] P. Kumar, K. B. Mirza, K. Choudhury, M. Cucchiarini, H. Madry, P. Shukla, *Adv. Funct. Mater.* **2021**, *31*, 2009663.
[176] H. Tan, Q. Tao, I. Pande, S. Majumdar, Fu Liu, Y. Zhou, P O. Å. Persson, J. Rosen, S. van Dijken, *Nat. Commun.* **2020**, *11*, 1369.
[177] P. Iqbal, J. A. Preece, P. M. Mendes, In: *Supramolecular chemistry: from molecules to nanomaterials*, (Eds: J. W. Steed, P. A. Gale), Wiley, Oxford, **2012**.
[178] M. Mastrangeli, M. Perego, *Adv. Mater. Interfaces* **2020**, *7*, 2000182.
[179] Q. Xu, Y. Lv, C. Dong, T. S. Sreeprased, A. Tian, H. Zhang, Y. Tang, Z. Yu, N. Li, *Nanoscale* **2015**, *7*, 10883.
[180] C. Li, J. Yang, W. He, M. Xiong, X. Niu, X. Li, D.-G. Yu, *Adv. Mater. Interfaces* **2023**, *10*, 2202160.
[181] K. Ni, Z. Wang, *Adv. Funct. Mater.* **2023**, *33*, 2213350.
[182] X. Lou, Y. Huang, X. Yang, H. Zhu, L. Heng, F. Xia, *Adv. Funct. Mater.* **2020**, *30*, 1901130.
[183] R. Luthfikasari, T. V. Patil, D. K. Patel, S. D. Dutta, K. Ganguly, M. M. Espinal, K.-T. Lim, *Small* **2022**, *18*, 2201417.
[184] S. Y. Kim, R. Thangam, N. Kang, H. Hong, C. Kim, S. Lee, S. Son, H.-J. Lee, K.-R. Tag, S. Min, D. Jeong, J. Hwang, K. Kim, D. Kim, Y. Kim, J. Joo, B. H. Kim, Y. Zhu, S.-G. Park, H.-C. Song, W. Sun, J.-P. Ahn, W. Y. Jang, R. Paulmurugan, H.-K. Kim, J. S. Kim, H. Kang, *Adv. Funct. Mater.* **2023**, *33*, 2215166.
[185] J. Wosik, W. Chen, K. Qin, R. M. Ghobrial, J. Z. Kubiak, M. Kloc, *Biophys. J.* **2018**, *114*, 2001.
[186] D. Huang, K. Xu, X. Huang, N. Lin, Y. Ye, S. Lin, J. Zhang, J. Shao, S. Chen, M. Shi, X. Zhou, P. Lin, Y. Xue, C. Yu, X. Yu, Z. Ye, K. Cheng, *Small* **2022**, *18*, 2203680.
[187] J. Wu, J. Zhu, Q. Wu, Y. An, K. Wang, T. Xuan, et al., *ACS Appl. Mater. Interfaces* **2021**, *13*, 2230.
[188] G. Bae, Y. S. Jeon, M. J. Ko, Y. Kim, S.-B. Han, R. Thangam, W. Kim, H. J. Jung, S. Lee, H. Choi, S. Min, H. Hong, S. Park, S. Y. Kim, K. D. Patel, N. Li, J. E. Shin, B. C. Park, H. S. Park, J. H. Moon, Y. J. Kim, U. K. Sukumar, J.-J. Song, S. Y. Kim, S.-H. Yu, Y. C. Kang, S. Park, S. M. Han, D.-H. Kim, K.-B. Lee, Q. Wei, L. Bian, R. Paulmurugan, Y. K. Kim, H. Kang, *Adv. Funct. Mater.* **2021**, *31*, 2103409.
[189] R. Thangam, M. S. Kim, G. Bae, Y. Kim, N. Kang, S. Lee, H. J. Jung, J. Jang, H. Choi, N. Li, M. Kim, S. Park, S. Y. Kim, T. M. Koo, H. E. Fu, Y. S. Jeon, A. Ambriović-Ristov, J-J. Song, S. Y. Kim, S. Park, Q. Wei, C. Ko, K-B. Lee, R. Paulmurugan, Y. K. Kim, H. Kang, *Adv. Funct. Mater.* **2021**, *31*, 2008698.
[190] A. Vinhas, M. T. Rodrigues, A. Gonçalves, R. Reis, M. E. Gomes, *Acta Biomater.* **2020**, *117*, 235.
[191] K. Marycz, A. Smieszek, K. Marcinkowska, M. Sikora, E. Turlej, P. Sobierajska, et al., *Int. J. Nanomed.* **2021**, *16*, 3429.
[192] H. Choi, G. Bae, C. Khatua, S. Min, H. J. Jung, N. Li, I. Jun, H.-W. Liu, Y. Cho, K.-H. Na, M. Ko, H. Shin, Y. H. Kim, S. Chung, J.-J. Song, V. P. Dravid, H. Kang, *Adv. Funct. Mater.* **2020**, *30*, 2001446.
[193] F. Xue, S. Zhu, Q. Tian, R. Qin, Z. Wang, G. Huang, S. Yang, *J. Colloid Interface Sci.* **2023**, *629*, 554.
[194] X. Wang, Y. Wang, Z. Xue, W. Wan, Y. Li, H. Qin, et al., *J. Colloid Interface Sci.* **2023**, *636*, 388.

[195] S. Hao, J. Meng, Y. Zhang, J. Liu, X. Nie, F. Wu, Y. Yang, C. Wang, N. Gu, H. Xu, *Biomaterials* **2017**, *140*, 16.
[196] H. Wu, H. Dong, Z. Tang, Y. Chen, Y. Liu, M. Wang, X. Wei, N. Wang, S. Bao, D. Yu, Z. Wu, Z. Yang, X. Li, Z. Guo, L. Shi, *Biomaterials* **2023**, *293*, 121990.
[197] P. Li, J. Xu, Q. Shi, J. Wang, W. Zhang, L. Zheng, M. Wang, Y. Fan, *Adv. Wound Care* **2023**, *12*, 498.
[198] C. He, S. Sun, Y. Zhang, F. Xie, S. Li, *Oncoimmunology* **2021**, *10*, 1897295.
[199] J. Gu, C. Wu, X. He, X. Chen, L. Dong, W. Weng, K. Cheng, D. Wang, Z. Chen, *ACS Biomater. Sci. Eng.* **2023**, *9*, 2615.
[200] A. Vinhas, A. F. Almeida, A. I. Gonçalves, M. T. Rodrigues, M. E. Gomes, *Int. J. Mol. Sci.* **2020**, *21*, 5441.
[201] Y. Kong, F. Liu, B. Ma, J. Duan, W. Yuan, Y. Sang, L. Han, S. Wang, H. Liu, *Adv. Sci.* **2021**, *8*, 2100962.
[202] V. Ballotta, A. Driessen-Mol, C. V. Bouten, *Biomaterials* **2014**, *35*, 4919.
[203] S. Wang, H. Yan, B. Fang, C. Gu, J. Guo, P. Qiu, N. Song, W. Xu, J. Zhang, X. Lin, X. Fang, *Biomaterials* **2022**, *285*, 121519.
[204] Q. Zhao, M. Shi, C. Yin, Z. Zhao, J. Zhang, J. Wang, K. Shen, L. Zhang, H. Tang, Y. Xiao, Y. Zhang, *Nano-Micro Lett.* **2021**, *13*, 1.
[205] R. Luo, Y. Liang, J. Yang, H. Feng, Y. Chen, X. Jiang, Z. Zhang, J. Liu, Y. Bai, J. Xue, S. Chao, Y. Xi, X. Liu, E. Wang, D. Luo, Z. Li, J. Zhang, *Adv. Mater.* **2023**, *35*, 2208395.
[206] J. Wang, J. Lin, L. Chen, L. Deng, W. Cui, *Adv. Mater.* **2022**, *34*, 2108325.
[207] H. Lei, D. Fan, *Adv. Sci.* **2022**, *9*, 2201425.
[208] Z.-C. Hu, J.-Q. Lu, T.-W. Zhang, H.-F. Liang, H. Yuan, D.-H. Su, W. Ding, R.-X. Lian, Y.-X. Ge, B. Liang, J. Dong, X.-G. Zhou, L.-B. Jiang, *Bioact. Mater.* **2023**, *22*, 1.
[209] J. Park, N. Jeon, S. Lee, G. Choe, E. Lee, J. Y. Lee, *Chem. Eng. J.* **2022**, *446*, 137344.
[210] T. Kreller, J. Zimmermann, U. van Rienen, A. Boccaccini, A. Jonitz-Heincke, R. Detsch, *Biomater. Adv.* **2023**, *146*, 213285.
[211] K. Battiston, R. Labow, C. Simmons, J. Santerre, *Acta Biomater.* **2015**, *24*, 74.
[212] P. Zhang, X. Liu, P. Guo, X. Li, Z. He, Z. Li, M J. Stoddart, S. Grad, W. Tian, D. Chen, X. Zou, Z. Zhou, S. Liu, *Bioact. Mater.* **2021**, *6*, 3097.
[213] T. T. Y. Han, J. T. Walker, A. Grant, G. A. Dekaban, L. E. Flynn, *Front. Bioeng. Biotechnol.* **2021**, *9*, 642465.
[214] P.-P. Zhao, Y.-W. Ge, X.-L. Liu, Q.-F. Ke, J.-W. Zhang, Z.-A. Zhu, Y.-P. Guo, *Chem. Eng. J.* **2020**, *381*, 122694.
[215] M. Wu, H. Liu, Y. Zhu, F. Chen, Z. Chen, L. Guo, P. Wu, G. Li, C. Zhang, R. Wei, L. Cai, *Small* **2023**, *19*, 2300111.
[216] L. Zhou, L. Zhou, C. Wei, R. Guo, *Carbohydr. Polym.* **2022**, *291*, 119558.
[217] M. Guo, S. Wang, Q. Guo, B. Hou, T. Yue, D. Ming, et al., *ACS Appl. Mater. Interfaces* **2021**, *13*, 18423.
[218] N. Xu, Y. Gao, Z. Li, Y. Chen, M. Liu, J. Jia, R. Zeng, G. Luo, J. Li, Y. Yu, *Chem. Eng. J.* **2023**, *466*, 143173.
[219] J. Shao, J. Li, L. Weng, K. Cheng, W. Weng, Q. Sun, et al., *ACS Biomater. Sci. Eng.* **2023**, *9*, 2483.
[220] E. E. van Haaften, T. B. Wissing, N. A. Kurniawan, A. I. Smits, C. V. Bouten, *Adv. Biosyst.* **2020**, *4*, 1900249.
[221] https://www.fda.gov/medical-devices (accessed: April, 2024).

Keya Ganguly is a postdoctoral research associate at Kangwon National University. She received her doctoral degree from the Department of Biosystems Engineering at Kangwon National University, South Korea. She received her Master's degree from Presidency University, India. Her research interest is developing a (multi)stimuli-assisted scaffolding platform for tissue engineering.

Rachmi Luthfikasari received her Master's degree from the Department of Biosystems Engineering at Kangwon National University, South Korea. She received her Bachelor's degree in biology from the University of Indonesia, Indonesia. Her research interest is biomimetic material and its application in tissue engineering.

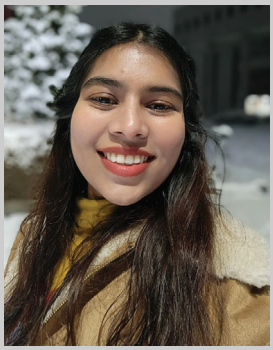

Aayushi Randhawa is a doctoral student in biosystems engineering at Kangwon National University, South Korea. She received her Master's degree from Bangalore University, India. Her research interest is developing stimuli-dependent regenerative therapies for healing damaged tissues.

Sayan Deb Dutta is a former postdoctoral research associate at Kangwon National University. He received his doctoral degree from the Department of Biosystems Engineering at Kangwon National University, South Korea. He reviewed his Master's degree from the University of Kalyani, India. His research interest spanned the synthesis of multifunctional nanomaterials for 3D printing and nanotheranostic applications for tissue engineering.

Tejal V. Patil is a doctoral student of biosystems engineering at Kangwon National University, South Korea. She received her Master's degree from the Institute of Chemical Technology, Mumbai, India. Her research interest is developing biomaterials for application in bacteria eradication and tissue regeneration.

Rumi Acharya is a doctoral student in biosystems engineering at Kangwon National University, South Korea. She received her Master's degree from Guru Ghasidas University, India. Her research interests are nanobiosensors and magnetogenetic therapy on cellular targets.

Ki-Taek Lim is a professor at the Department of Biosystems Engineering at Kangwon National University, South Korea. He received his doctoral degree from Seoul National University, South Korea, and joined as a postdoctoral research fellow at the University of Arkansas, USA. He has a strong knowledge of mechatronics and regenerative medicines. His research focuses on developing the bio-nanorobotics system with novel bioreactors and stem cell cultures for tissue-engineering applications.